


Scenarios of fish waste deposition at the sub-lagoon scale: a modelling approach for aquaculture zoning and site selection

Killian Chary ^{1*}, Myriam D. Callier¹, Denis Covès¹, Joël Aubin², Julien Simon³, and Annie Fiandrino⁴

¹MARBEC, Univ Montpellier, IRD, CNRS, Palavas-les-Flots, Ifremer 34250, France

²UMR 1069 INRA AGROCAMPUS-OUEST SAS, Rennes 35042, France

³Ifremer, Laboratoire de Technologie et de Biologie Halieutiques, RBE/STH/LTBH, Lorient 56100, France

⁴MARBEC, Univ Montpellier, IRD, CNRS, Sète, Ifremer 34200, France

*Corresponding author: tel: +33 4 67 13 04 24; e-mail: Killian.Chary@ifremer.fr or Killian.Chary@gmail.com.

Chary, K., Callier, M. D., Covès, D., Aubin, J., Simon, J., and Fiandrino, A. Scenarios of fish waste deposition at the sub-lagoon scale: a modelling approach for aquaculture zoning and site selection. – ICES Journal of Marine Science, 78: 922–939.

Received 13 August 2020; revised 3 December 2020; accepted 5 December 2020; advance access publication 19 January 2021.

Spatial planning, including zoning and site-selection steps, is necessary to determine locations that minimize environmental impacts of aquaculture and respect ecosystem carrying capacities. This study aimed to analyse potential benthic waste deposition in a broad range of fish farming situations to facilitate zoning. To this end, we simulated waste dispersion for 54 aquaculture scenarios combining three red drum (*Sciaenops ocellatus*) farm types (Small, Medium, and Large) based on real farm characteristics and 36 sites with contrasting hydrodynamics in Mayotte's North-East Lagoon. Key forcing variables and parameters of the particle-dispersion model for farms (layout and solid waste fluxes), species (feed- and faeces-settling velocities) and sites (depth and barotropic currents) were obtained. From the outputs of the 54 simulations, relationships between hydrodynamic regimes and deposition rates, area of influence and distance of influence of the farm were analysed. Critical limits of current intensity that reduced deposition rate below selected deposition thresholds were identified. For instance, to prevent deposition rates greater than $12 \text{ kg solids m}^{-2} \text{ year}^{-1}$, the mean current intensity should exceed 10.2 and 6.8 cm s^{-1} for Medium and Large farms, respectively. The study confirmed that production level is not the main factor that influences deposition rates; instead, management of the entire farm (cage position, distance between cages) must be considered to predict impacts more accurately and guide site selection.

Keywords: aquaculture zones, carrying-capacity, environmental impact, hydrodynamics, NewDEPOMOD, particle dispersion, red drum, scenario analysis

Introduction

Aquaculture continues to grow faster than other major food production sectors, and its global production of food products (excluding aquatic plants) peaked at 80 million t in 2016, of which mariculture (i.e. aquaculture in marine environments) produced 36% (FAO, 2018). Mariculture has high potential for growth given the large amount of marine area available, which far exceeds the area required to meet foreseeable seafood demand (Gentry *et al.*, 2017b). In terms of volume, mariculture produces mainly high-value finfish but also seaweed, bivalve molluscs, and

crustaceans (Bostock *et al.*, 2010; FAO, 2018). Historically, mariculture has developed in coastal waters (i.e. intertidal areas, estuaries, and sheltered bays) to benefit from calm water and easy access to cages (Gentry *et al.*, 2017a). However, with the concomitant increase in the scale and efficiency of rearing technologies and the competition for space with other activities (e.g. fisheries, energy production, conservation, tourism, military activities, transport) in coastal areas, the sector is expected to expand to more remote locations (Marra, 2005). Since the sector will continue to grow and expand to new areas, planning and organizing

future aquaculture development is necessary to reduce conflicts with other activities and to apply a sustainable development and ecosystem approach to aquaculture (Soto *et al.*, 2008; Sanchez-Jerez *et al.*, 2016).

Applying spatial planning to aquaculture consists of two key steps: (i) identifying suitable areas for aquaculture development (i.e. zoning) and (ii) determining the location of specific sites (i.e. site selection). To define broad areas suitable for the activity, aquaculture zoning needs to consider a variety of criteria, including biophysical requirements for farmed species and systems (e.g. water quality, temperature, suitable depth, and currents), environmental (e.g. proximity to sensitive habitats), social (e.g. visual impact, adjacent human activities), and economic (e.g. access to roads and services) [see Aguilar-Manjarrez *et al.* (2017) for a more extensive list]. Zoning can provide general recommendations about species that can be cultured efficiently in a particular area and broad indications of the production systems that are best suited. Site selection aims to identify the most appropriate locations for new farms within zones depending on the farms' characteristics (e.g. species, infrastructure, scale, practices) (Ross *et al.*, 2013). An environmental impact assessment is generally performed to ensure that the planned farm would not exceed the site's ecological carrying capacity (Aguilar-Manjarrez *et al.*, 2017).

Ecological carrying capacity in aquaculture is generally defined as the level of aquaculture production that can be produced without changing the environment significantly (McKindsey *et al.*, 2006; Ross *et al.*, 2013). Potential impacts on the environment include near-field effects (e.g. benthic impact, water quality impact, habitat modification), which occur near the farm, and far-field effects (e.g. nutrient enrichment, food web dynamics, spread of disease, and pathogens) (Weitzman and Filgueira, 2019). For fin-fish mariculture, ecological carrying capacity is generally focused on near-field effects, especially benthic impact. Thus, ecological carrying capacity is often considered primarily as the capacity of a site or ecosystem to support solid-waste (i.e. fish faeces and uneaten feed) accumulation on the seabed (Weitzman and Filgueira, 2019) and by comparing potential impacts to environmental quality standards (EQS) (Stigebrandt, 2011). Specific EQS can be fixed within an acceptable zone of effect (AZE) for aquaculture, and impacts should not irreversibly compromise the ecosystem services provided (GFCM, 2012). Deposition on the seabed of large amounts of organic matter in the vicinity of a fish farm may cause eutrophication of water bodies, promote plankton blooms, and decrease oxygen concentrations, which may impact surrounding ecosystems (Wu, 1995; Fernandes *et al.*, 2001). Benthic impacts depend upon the characteristics and quantity of waste released from a farm, its dispersion (influenced by site hydrodynamics, i.e. currents and depth) and ultimately ecosystem sensitivity (driven by its biotic and abiotic characteristics), all of which determine waste accumulation on the seabed and the response of the benthic ecosystem. Due to the multifactorial nature of ecological carrying capacity, simulation models are often developed to represent the multiplicative and cumulative nature of the physical and ecological processes involved (Byron and Costa-Pierce, 2013).

Particle-dispersion models aim to simulate dispersion of particulate waste from a farm, its accumulation on the seabed and sometimes the resulting biogeochemical response of sediment. A number of dispersion models has been developed in the past decade, such as those developed by Cromey *et al.* (2002), Stigebrandt *et al.* (2004), Corner *et al.* (2006), or Jusup *et al.*

(2009). These models have been used in both research and decision-making to estimate ecological carrying capacities of fin-fish farms. DEPOMOD, well known for its extensive use and good accuracy for a variety of environments, has been continually improved to meet increasingly specific requirements. Initially developed to assess impacts of Atlantic salmon (*Salmo salar*) culture in Scotland, it has been then adapted into different versions (CODMOD, MERAMOD, MACAROMOD, TROPOMOD) for Atlantic cod (*Gadus morhua*) farming in the Atlantic Ocean (Cromey *et al.*, 2009); seabream (*Sparus aurata*) and seabass (*Dicentrarchus labrax*) farming in the Mediterranean Sea (Cromey *et al.*, 2012); milkfish (*Chanos chanos*) farming in the Philippines (Aquapark, 2015; White and Lopez, 2017); meagre (*Argyrosomus regius*) farming in Macaronesia (archipelagos in the North-East Atlantic) (Riera *et al.*, 2017), and even shellfish farming in the North Atlantic (Weise *et al.*, 2009). Recently, a new version of the model (NewDEPOMOD) was released (Black *et al.*, 2016). While some reports mentioned that it performed well (Black *et al.*, 2016; Hadley *et al.*, 2017), it has yet to be validated in a peer-reviewed study.

Knowledge gaps are now related to understanding the variability in benthic impact across space, hydrodynamic regimes, and farm characteristics. Until recently, this variability in benthic impact was studied mainly with statistical models to highlight possible correlations between observed benthic effects on operating farms and farm or site characteristics (Giles, 2008; Borja *et al.*, 2009; Mayor *et al.*, 2010). Although useful, these studies are limited to real farm and site cases, whose potential benthic impacts cannot be extrapolated to other conditions. Doing so requires using mechanistic particle-dispersion models and exploratory scenario analysis. In the past decade, several studies applied such models to a variety of hydrodynamic and farming conditions and/or scenarios (Cromey *et al.*, 2009, 2012; Lee *et al.*, 2016; Brigolin *et al.*, 2017; Riera *et al.*, 2017; White and Lopez, 2017). However, few have related differences in predicted and/or observed impacts to these varying factors (Keeley *et al.*, 2013; Chang *et al.*, 2014). In New Zealand, Keeley *et al.* (2013) examined benthic impacts of five salmon farms (production level not specified) with contrasting flow regimes (depths of 27–40 m and mean current intensities at mid-depth of 3–20 cm s⁻¹). The authors distinguished two relationships between deposition rate and enrichment level depending on current intensity and sediment sensitivity to resuspension. In Canada, Chang *et al.* (2014) compared benthic impacts of six salmon farms that varied in size (stocked biomass of 0–1770 t at the time of sampling) and hydrodynamic regimes (depths of 15–22 m and mean current intensities of 5–14 cm s⁻¹). They found no consistent relationship between current speed and areas with high deposition rates, and assumed that this lack of relationship was due to the shallow depths and thus short settling times of solid waste. These relationships can help specify what range and combination of depth and current intensity may minimize risks of impacts.

However, these two studies did not describe farms in detail, which prevents one from inferring relationships between their characteristics (e.g. scales, rearing technologies, practices) and impact patterns, and makes the representativeness of the farms unclear. Identifying the farm types in a given area is also necessary, since fish farming does not always follow a production continuum, but sometimes has discrete production levels that can be attained at different farm scales using specific infrastructure and technology, which influence deposition footprints strongly.

Moreover, the few hydrodynamic regimes examined and their unknown spatial representativeness may limit the utility of these relationships for zoning or site selection. A broad view and exploratory analysis that considers the main types of aquaculture (e.g. practices, technologies, scales) and variability in hydrodynamic regimes in a given zone is required to test effects of different scenarios on benthic deposition and provide a predictive tool for decision-makers.

The aim of the present study was to develop and apply a method to estimate dispersion and primary benthic waste deposition from different types of fish farms in a broad range of hydrodynamic regimes to facilitate zoning and site selection. We applied this method to red drum (*Sciaenops ocellatus*) farming in the North-East (NE) lagoon of the Mayotte Islands. Specifically, we (i) defined three main farms types (Small, Medium, Large) based on real farm characteristics, (ii) analysed the hydrodynamic regime of Mayotte’s NE Lagoon to determine 36 sites with contrasting regimes, (iii) simulated waste dispersion and deposition for 54 scenarios (combining farm types and sites), and (iv) established relationships between hydrodynamic regimes and waste deposition metrics (i.e. maximum deposition rate, area under farm influence, and maximum distance of impact).

Material and methods

Analysis framework

We developed an analysis framework to aid zoning and site selection for aquaculture based on predicting environmental impacts of fish farming in a broad range of explorative scenarios (i.e. situations or developments that are considered possible) (Börjeson et al., 2006). Its five steps (Figure 1) involved the use of three models (Figure 2):

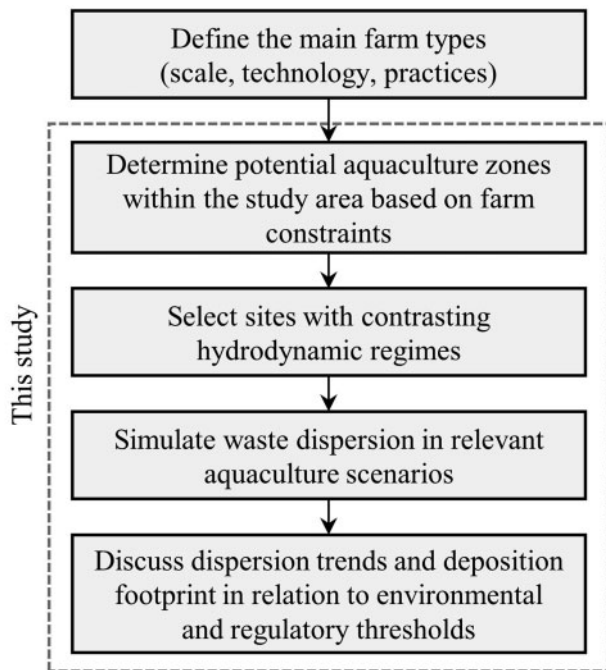


Figure 1. Framework developed to estimate waste deposition of fish farming in Mayotte’s North-East Lagoon.

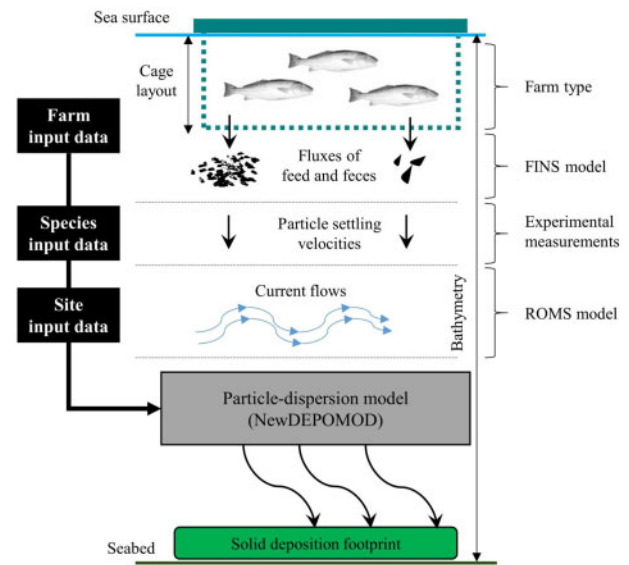


Figure 2. Description of the models used and their input data. Dispersion of fish farming waste was predicted with the NewDEPOMOD model using feed and faeces fluxes predicted by the FINS model (Chary et al., 2019), particle-settling velocity data and current flows in Mayotte’s North-East Lagoon simulated with ROMS (Chevalier et al., 2017).

- (1) The main farm types in Mayotte were defined based on surveys, and fluxes of solid waste (faeces and uneaten feed) from each farm type were estimated using the FINS farm-scale model. This step was performed in a previous study (Chary et al., 2019).
- (2) Zones where aquaculture could be developed within the study area were determined as a function of physical (depth) and logistical (distance from the coast) constraints of the farming systems.
- (3) Contrasting site profiles, including different hydrodynamic regimes (barotropic currents and depth) were selected within aquaculture zones using a clustering method. Simulations of hourly barotropic currents were obtained for each selected site from the three-dimensional hydrodynamic Regional Ocean Modeling System (ROMS) (Chevalier et al., 2017).
- (4) Dispersion of fish farming waste was simulated for all relevant farm and site combinations using NewDEPOMOD (Black et al., 2016).
- (5) The factors that most influenced predicted extents of deposition on the seabed (i.e. deposition footprints) were examined, and the results interpreted in light of thresholds of deposition rates (based on the literature) to develop recommendations for zoning and site selection.

Application to the Mayotte case study and farm types

Case study

Mayotte is part of the Comoro Islands, located in the northern end of the Mozambique Channel, 300 km northwest of Madagascar and 450 km east of Mozambique. Mayotte (374 km²) is composed of two main islands—Petite-Terre and Grande-Terre—enclosed in a 1500 km² lagoon created by a double-reef system. The second and external reef is discontinuous and forms

three main complexes: the NE reef, the reefs south of Petite-Terre, and the South reef. A marine nature park covers all Mayotte's EEZ, including the entire lagoon. The park pursues several objectives, including protection of the park and sustainable development of marine activities, including aquaculture.

We studied the northeastern part of the lagoon (NE Lagoon, 25 km long, 2–10 km wide, Figure 3), where the first and largest (production capacity of 400 t year⁻¹) fish farm in Mayotte was established in 1999 and where a plan for a large-scale farm (production capacity of 1500 t year⁻¹) is currently being investigated. The NE Lagoon has two inner passages connecting adjacent lagoons (Chevalier *et al.*, 2017). Hydrodynamics within the NE Lagoon are driven mainly by the tide, with typical mesotidal variations ranging from 0.8–2.7 m and up to 4 m during extreme tides (Dinhut *et al.*, 2008; Chevalier *et al.*, 2017). The lagoon has

a relatively weak swell due to Mayotte's sheltered location in the Mozambique Channel and to the presence of the double-reef system (De La Torre *et al.*, 2008). The dominating SE–SSW winds (50% of all winds) are relatively weak, reaching 4.3 m s⁻¹, but tropical storms or cyclones can bring high winds from January to April (Jeanson *et al.*, 2013). The lagoon's water temperature is relatively stable and high (26–29°C), which can increase the growth potential of aquaculture species.

Farm types

The fish farming sector in Mayotte produces mainly red drum, and the range of possible farming conditions in Mayotte was described in a previous study by three main farm types according to farm scale, production objectives, and technical and socio-

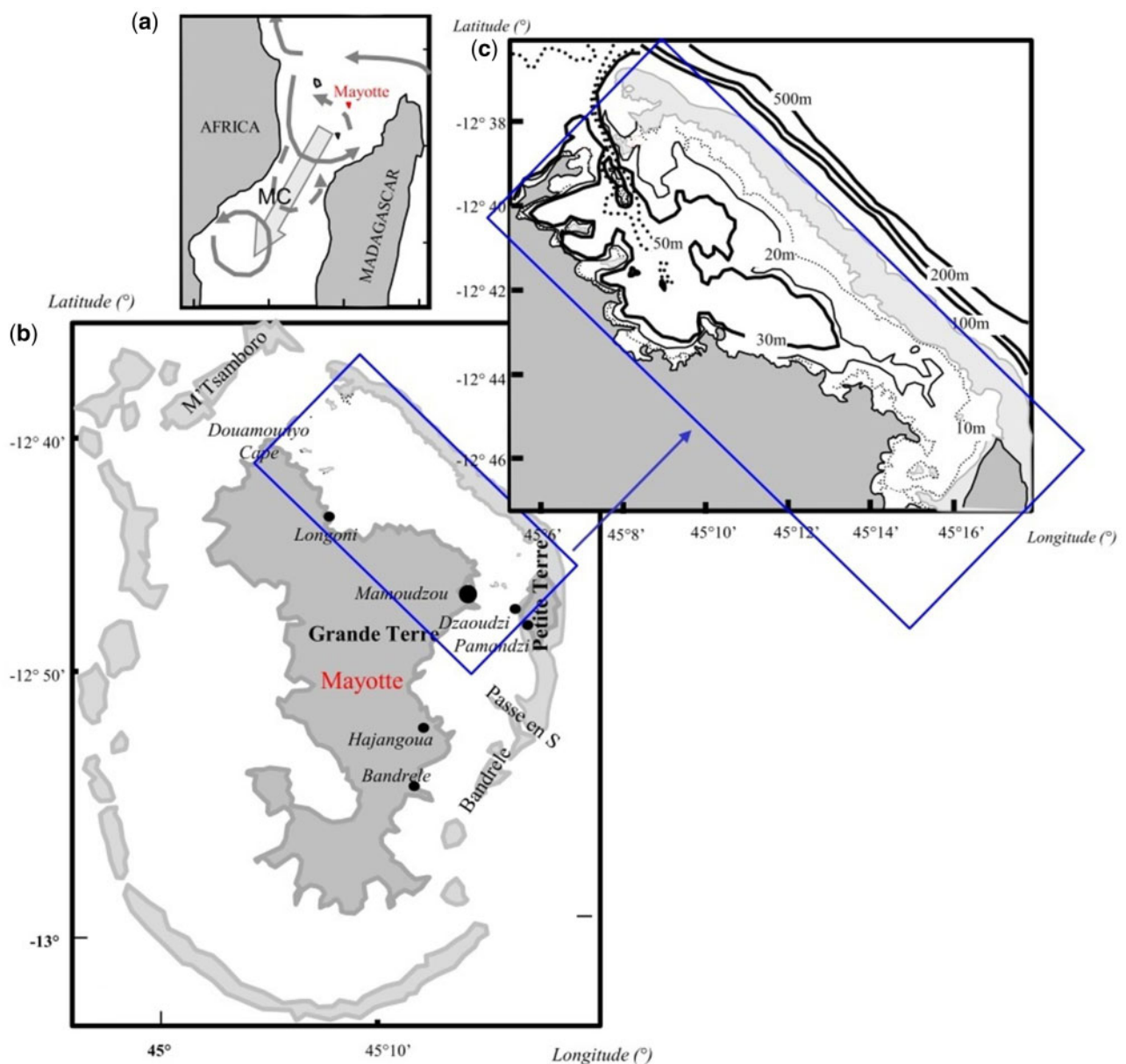


Figure 3. Study area: (a) Location of Mayotte in the Mozambique Channel (MC) (b) location and scope of the North-East Lagoon (c) depth in the North-East Lagoon. Modified from Chevalier *et al.* (2017).

economic criteria (Chary et al., 2019). Possible fish farming systems in the area were categorized from a survey of existing and planned farms. These categories were used to build three hypothetical farm scenarios: Small, Medium, and Large farms. The farm scenarios were distinguished by specific production systems (farm scale and associated technological level), production objectives, and rearing practices. The Small farm produced 23 t year⁻¹ and had simple aquaculture technology (rectangular floating plastic cages). Because the Small farm required sheltered areas and easily accessible sea-cage facilities (to facilitate farming operations and security), it was restricted to nearshore coastal areas. The Medium farm's system was an upscaled version of that for the Small farm, with similar design and technology but more cages, which can produce 299 t year⁻¹. The use of safer and larger boats, however, and of surveillance cameras allowed the Medium farm to sit further from the coast. The Large farm's system (2079 t year⁻¹) had more advanced technology and large service vessels to store feed and house employees. Thus, its cages were assumed to be permanently accessible for farming operations and security. See Table 1 for a summary of farm characteristics (i.e. dimension, number of cages, feed inputs, stocking density); more details can be found in Chary et al. (2019).

Aquaculture scenarios

Explorative aquaculture scenarios were built to examine the potential benthic waste deposition footprint of the three farming systems in the study area. First, preliminary zoning based on farm siting constraints (site depth and distance from coast) identified zones where at least one of these three farming systems could be established. Then, sites with contrasting hydrodynamics were selected in each of these zones. Finally, relevant aquaculture scenarios were built by defining relevant combinations of each farming system and site.

Definition of aquaculture zones

Broad zones suitable for farms were defined based on logistical and economic constraints of the farm types and their technologies. Site depth and distance from the coast are the two physical factors used most often to describe sites in offshore aquaculture (Froehlich et al., 2017) and, more generally, are criteria commonly used to categorize sites (Holmer 2010; Lovatelli et al. 2013). A minimum distance between nets and the seabed is required to eliminate abrasion, which may damage the nets and cause fish escapes and high maintenance costs. Thus, it is generally recommended that the water be ca. twice as deep as the total net depth (Belle and Nash, 2008; Karakassis, 2013; Cardia et al., 2017). Consequently, minimum depths of 8, 26, and 26 m are

necessary for the Small, Medium, and Large farms, respectively. Distance from the coast tends to determine the cost-effective area of mariculture development and the degree of accessibility under varying environmental conditions (Kapetsky et al., 2013). Aquaculture sites are usually divided into coastal (<500 m from the coast), off-coast (500–3000 m), and offshore zones (>3000 m) (e.g. Holmer 2010; Lovatelli et al. 2013). These distances were used to set the maximum distance at which each farm type could be established: 500 m for Small farms, 3000 m for Medium farms, and no limit for the Large farm. According to depth and distance constraints, the following basic zoning was then adopted:

- Coastal: areas <500 m from the coastline with water at least 8 m deep.
- Off-coast: areas 500–3000 m from the coastline with water at least 26 m deep.
- Deep lagoon: areas >3000 m from the coastline with water at least 26 m deep.

Selection of sites with contrasting hydrodynamic regimes

To characterize hydrodynamic spatial variability in the NE Lagoon and select contrasting sites, we used predictions from ROMS (Chevalier et al., 2017), which was initially used to study hydrodynamic regimes caused by the tide this part of the lagoon and subsequently validated. ROMS includes bathymetry from Litto3D Mayotte (SHOM, 2019) to generate a horizontal 275 km² regular grid with a 250-m cell resolution (9844 cells) and a vertical discretization into ten levels with surface refinement based on a topography-following coordinate (σ coordinate). Since this cell size (62 500 m²) was similar to the size of the leased area of the Large farm, we assumed that one entire grid cell could be considered as a potential site for aquaculture. Hourly horizontal current fields at ten depths over 15 days were predicted by ROMS for each potential site and used (i) to characterize spatial variability in hydrodynamics at the sub-lagoon scale and select contrasting sites and (ii) as horizontal current forcing for particle-dispersion simulations.

A four-step procedure was followed to select sites with contrasting hydrodynamic regimes:

- (1) Coastal, off-coast, and deep lagoon zones were collated in three distinct datasets containing 213 (2.2% of the cells in the grid), 735 (7.5%), and 378 (3.8%) sites, respectively. Hourly three-dimensional current fields from these 1326 potential sites were extracted from ROMS results over the 15-day spring-to-neap tidal cycle.

Table 1. Description of the Small, Medium, and Large red drum farm types.

Characteristic	Small	Medium	Large
Annual production (t)	23	299	2079
Cage layout	6 rectangular (6 m L × 6 m W × 4 m H)	4 rectangular (7 m L × 7 m W × 8 m H)	6 circular (12 m D × 6 m H)
		6 rectangular (14 m L × 14 m W × 13 m H)	24 circular (20 m D × 12 m H)
Total area covered by cages (m ²)	216	1372	8218
Total sea surface area leased (m ²)	274	1708	64 400
Maximum stocking density (kg m ⁻³)	20	20	20
Annual feed input (t)	35	529	3230

- (2) Hydrodynamic regimes at low tide (LT) and high tide (HT) were described by aggregated criteria that corresponded to duration (D_{LT} , D_{HT}), preferential direction (θ_{LT} , θ_{HT}), and barotropic current intensity averaged over D_{LT} and D_{HT} (I_{LT} , I_{HT}). The percentage of time the current was established in these two preferential directions over the 15-day spring-to-neap tidal cycle (% EC) was also calculated.
- (3) Principal component analysis (PCA) and hierarchical cluster analysis (HCA) were performed for each zone's dataset to distinguish different hydrodynamic regimes. Analysis was performed with the FactoMineR package (Le *et al.*, 2008) of R software (R Core Team, 2018) using five descriptive variables: % EC, I_{LT} , I_{HT} , D_{HT} , and depth (H). The PCA and HCA yielded three site clusters in each zone (total: 9 clusters) with the same general characteristics (Supplementary Table S1). In the first cluster, current was established less frequently (% EC = 75–87%) than in the other two clusters (% EC > 94%). In the second cluster, most barotropic currents had low intensity (I_{LT} and I_{HT} ranged from 3.4 to 5.2 cm s⁻¹), while in the third cluster, barotropic currents had higher intensity (5.3–14.9 cm s⁻¹). Depth was not a distinguishing criterion of site hydrodynamics in the study area in the PCA results.
- (4) Although depth did not distinguish hydrodynamics, it can influence waste dispersion by influencing the time required for particles in the water column to reach the seabed. Consequently, four subtypes of hydrodynamic regime with contrasting particle-dispersion potentials were defined in each cluster based on current intensity and depth: low intensity/low depth, low intensity/high depth, high intensity/low depth, and high intensity/high depth.

From this procedure, 12 sites (3 clusters × 4 contrasting regimes) were selected in each of the 3 zones, which yielded a total of 36 sites that represented the variability in hydrodynamics of the NE Lagoon.

Definition of relevant aquaculture scenarios

To build aquaculture scenarios, relevant combinations of three farm types (Small, Medium, or Large) and the 36 potential sites to simulate were selected based on depth and distance from the coast. In the coastal zone, the 12 sites were appropriate for Small farms (depth >8 m), but only 3 of them were deeper than 26 m and thus appropriate for Medium and Large farms. In the off-coast zone, only Medium and Large farms could be established at the 12 sites selected, because the coast was too distant for Small farms. Likewise, in the deep zone, only Large farms could be established at the 12 sites. Thus, waste dispersion and deposition were simulated for 54 scenarios (12, 15, and 27 for Small, Medium, and Large farms, respectively).

Models: structure, inputs, and key forcing variables

For each aquaculture scenario, a finfish farm-scale model (FINS; Chary *et al.* 2019) was used to simulate waste fluxes, and a particle-dispersion model (NewDEPOMOD, version 20181109-125931-1541605374) was used to simulate waste dispersion and the deposition footprint. The structure of the models and their associated input data and key forcing variables are described below (Figure 2).

Waste fluxes simulated with FINS

FINS simulates farm production, feed requirements, and particle waste fluxes (FINS; Chary *et al.* 2019). The model combines farm production (individual-based growth model) and waste emission (nutrient mass-balance model) modules. FINS calculates feed inputs daily from feeding rate data given as a percentage of the cage's fish biomass, which varies over time as a function of fish growth and rearing practices. Under routine farming conditions, estimated mean daily feed inputs were 1.68, 0.82, and 1.38% for Small, Medium, and Large farms, respectively. Calculated feed inputs include a loss fraction that represents uneaten feed. Uneaten feed can vary greatly, due to many factors (e.g. feeding practices, currents, temperature, species feeding behaviour) and is usually set to 1–5% in studies of waste dispersion from fish farms (Cromey *et al.*, 2002, 2009, 2012; Brigolin *et al.*, 2009; Keeley *et al.*, 2013; Riera *et al.*, 2017). A loss fraction of 5% of each daily feed input was set in this study, thus assuming a worst-case scenario. In the waste-emission module, waste fluxes were estimated using feed digestibility coefficients obtained from experiments with red drum fed commercial feeds (Nutrima[®] diets). FINS predicted daily solid waste fluxes (uneaten feed and faeces) from Small, Medium, and Large farms under routine farming conditions for a 1-year period. These daily solid fluxes were divided by 24 to obtain hourly emission time series (assuming continuous particle release) consistent with NewDEPOMOD input requirements.

Waste dispersion simulated with NewDEPOMOD

The general structure of NewDEPOMOD has the same four modules as those initially developed for DEPOMOD (Cromey *et al.*, 2002): (i) grid generation, (ii) particle tracking, (iii) resuspension, and (iv) benthic fauna response (benthic impacts). In this study, only the grid-generation and particle-tracking modules were used to obtain primary (initial) deposition footprints. Deposition and impact metrics were then calculated based on literature thresholds.

Grid-generation module

In the grid-generation module, domains covering an area of 4 km² with a horizontal resolution of 10 m × 10 m and a homogeneous flat seabed were generated, and cage layouts were set in the centre of the grid to build the 54 scenarios. The total area and the grid-cell resolution defined (Table 2) were a compromise among decreasing particle export out of the domains, providing sufficient spatial detail for the smallest cages (6 m × 6 m) and reducing computing time. We made the simplifying assumption of a homogenous flat seabed throughout the domain to ease comparison of deposition footprints predicted under different currents and depths. Simulated particles were released from random starting locations within each cage.

Particle-tracking module

Current intensity layer and time steps. In the particle-tracking module, we provided hourly horizontal current fields for three depth layers, as recommended by Hills *et al.* (2005): near-surface (3 m below the surface), near-bottom (3 m above the seabed), and mid-depth (midway between the surface and seabed). Tidal currents over a 15-day period (spring-to-neap tidal cycle) extracted from ROMS for the 36 grid cells, which corresponded to the 36 sites selected, were used. Currents were assumed to be the same throughout the domain, as required by NewDEPOMOD.

Table 2. NewDEPOMOD model settings for red drum (*S. ocellatus*) farming in Mayotte's North-East Lagoon.

Module or submodel	Input data	Value
Grid generation	Domain grid dimensions	2000 m × 2000 m
	Grid-cell resolution	10 m × 10 m
	Bathymetry	Flat and homogeneous
Particle tracking	Feed-pellet- and faeces-settling velocities	Values and distribution from this study
	Current intensity layers	Near-surface, mid-depth, near-bottom
	Current intensity time step	3600 s ^a
Turbulence	Random-walk model	Yes
	Horizontal dispersion coefficients k_x , k_y , and k_z	0.1, 0.1 and 0.001 m ² s ^{-1b}
Particle trajectory	Number of particles (of each particle type, per cage, per time step)	10 ^c
	Trajectory evaluation accuracy (model time step)	60 s ^a
Resuspension	Critical shear stress	2 ^c (= no resuspension)

Sources: ^aDefault values of Cromey et al. (2002); ^bDefault values of Gillibrand and Turrell (1997); ^cUser-defined in this study.

Feed pellet and faeces settling velocities. Feed pellet and faeces settling velocities are important species-specific parameters for modelling dispersion of aquaculture waste (Reid et al., 2009; Bannister et al., 2016; Broch et al., 2017). Since data on red drum waste-particle settling velocity were not available in the literature, an experiment was performed to predict waste dispersion accurately (see the Supplementary material for a full description). Briefly, we measured faeces-settling velocity rates of four commercial size categories (mean weight, small: 648 g, medium: 1152 g, large: 1913 g, very large: 3155 g) of cultured red drum and a range of red drum commercial feed (Nutrima[®] diet, i.e. NUTRImarine 1.2, 2.2, 3.2, 4.5, 6.0, and 9.0 mm pellets) commonly used on farms in Mayotte. The method was based on a previous experiment (Magill et al., 2006; Cromey et al., 2009; Perez et al., 2014), with the design improved to obtain fresh undamaged faecal material by connecting the fish tank directly to a settling column (Figure 4). Particle settling was recorded using an HD camera, and the videos were analysed with particle-tracking software to determine individual settling velocities of many fecal ($N = 2848$) and feed ($N = 186$) particles. Settling data were analysed statistically to determine theoretical distributions of feed- and faeces-settling velocities. In NewDEPOMOD, the settling velocity of simulated particles remains constant during the growing cycle; only the statistical distribution of velocities could be set. When modelling the entire growing cycle is the goal, as in the present study, mean values can be used because all fish size categories are usually grown simultaneously on a farm. Consequently, faeces-settling velocities for the four fish categories were pooled, and means and standard deviations (SD) were used in the dispersion model. Feed-settling velocities also needed to be pooled. In NewDEPOMOD, we used the mean and SD of settling velocities of the three largest pellets (4.5, 6.0, and 9.0 mm), which represented more than 90% of the annual mass of farm feed input under routine farming operations (Chary et al., 2019).

Resuspension module

Although the resuspension module in NewDEPOMOD has been updated since DEPOMOD and should simulate bed processes and resuspension mechanisms more accurately (Black et al., 2016), no studies of its application to or validation with other sites have been published yet. Using the resuspension module can change model outputs considerably (Chamberlain and Stucchi, 2007), and several studies that used DEPOMOD tended to turn

off resuspension to optimize model performances (Chamberlain and Stucchi, 2007; Cromey et al., 2012; Keeley et al., 2013; Chang et al., 2014). Consequently, we deactivated it as well. Deposition predictions were thus considered as “primary deposition footprints” (Keeley et al., 2013), i.e. deposition patterns and rates without any sediment reworking or mixing (e.g. resuspension, diagenesis).

Deposition metrics and impact threshold

Particulate waste deposition (i.e. kg solids m⁻² year⁻¹ in 100 m² grid cells) was simulated for the 54 scenarios with NewDEPOMOD. Deposition predictions were exported to

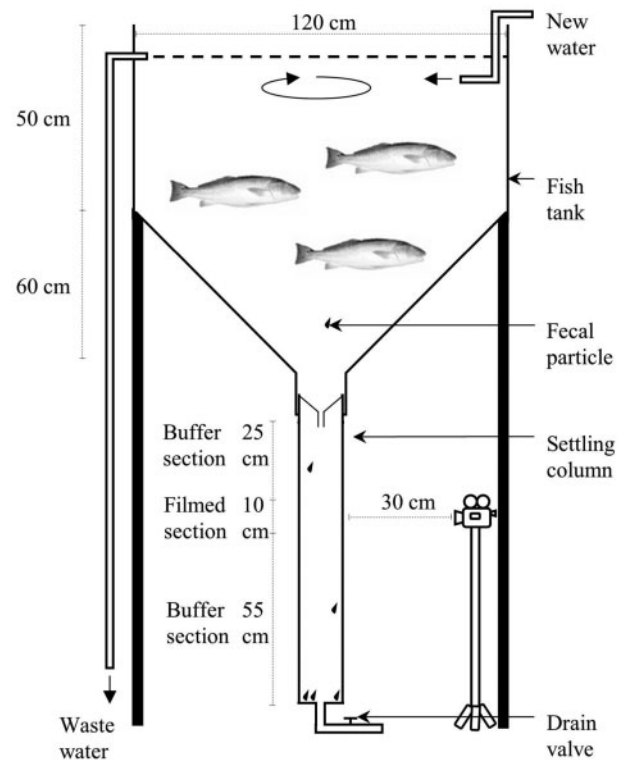


Figure 4. Side view of the setup for the faecal settling experiment. A fish tank was connected to a transparent settling column in which faecal particle sedimentation was recorded with a camera.

MATLAB version R2015b (The Mathworks Inc., 2015) to calculate metrics that characterized the deposition footprint: (i) the area under farm influence (AUI_F , m^2) at a given deposition rate (F) or range of rates (see below) and (ii) the maximum distance from cages at which F can be detected (DC_F , m).

Most studies defined environmental thresholds associated with fish farming in temperate environments and observed ecological effects across a broad range of deposition rates spanning two orders of magnitude (i.e. 0.1–10 kg solids $m^{-2} year^{-1}$) [reviewed in Keeley *et al.* (2013)]. Several studies defined the threshold of detectable impacts in the range of 0.01–2 kg solids $m^{-2} year^{-1}$ (Hargrave, 1994; Cromey *et al.*, 2002, 2012; Chamberlain and Stucchi, 2007; Keeley *et al.*, 2013). Since the relationship between solid fluxes and the biotic index available in the benthic module of NewDEPOMOD was developed and validated for temperate environments, it was not suitable to predict benthic impact in our study. Nonetheless, to illustrate how relationships between hydrodynamic regimes and deposition metrics developed in this study could be used to predict impact and help select sites, we used deposition rate thresholds for fish farms in tropical environments published in the literature, although information was scarce. Indeed, to our knowledge, only two studies have reported impact thresholds in tropical environments. Riera *et al.* (2017) observed significant decreases in sediment ecological status at deposition rates greater than 12 kg solids $m^{-2} year^{-1}$ for fish farms in Macaronesia, but they did not examine rates greater than 16 kg solids $m^{-2} year^{-1}$. In the Philippines, predicted deposition rates of 0.4–5.5, 5.5–27, and >27 kg solids $m^{-2} year^{-1}$ were categorized as moderate, high, and severe impacts, respectively (Aquapark, 2015; White and Lopez, 2017). Based on these values, three categories of impact were set as a function of F (kg solids $m^{-2} year^{-1}$) in the present study (Figure 5):

- $F \in [0.5; 12]$: detectable impact (D). We set the lower threshold to 0.5 instead of 0 because effects below it would be subtle and difficult to distinguish from the background of natural variability in nutrient enrichment, potentially resulting in less useful conclusions. For this range of deposition rate, AUI_D and DC_D thus represented the seabed area with detectable impacts and the farthest distance at which a detectable impact was

predicted in the domain, respectively. To ease comparison with other studies, this range is equivalent to 0.2–4.1 g C $m^{-2} d^{-1}$, assuming 45.5% C content in feed, 31.6% C content in faeces, and a 20:80 ratio of feed and faeces to total solids (Chary *et al.*, 2019).

- $F \in [12; 30]$: moderate (M) impact, equivalent to 4.1–10.3 g C $m^{-2} d^{-1}$
- $F \in [30; \max]$: severe (S) impact, equivalent to more than 10.3 g C $m^{-2} d^{-1}$

We thus calculated the AUI and DC for detectable (AUI_D and DC_D), moderate (AUI_M and DC_M), and severe (AUI_S and DC_S) impacts (Figure 5). The total AUI ($AUI_{F>0.5} = AUI_D + AUI_M + AUI_S$) and peak deposition in the grid of each simulation (F_{\max}) were also calculated.

Regression models were used to establish and test relationships between site hydrodynamic regimes [mean barotropic current intensity (i.e. mean of I_{LT} and I_{HT}) and depth as dependent variables] and the deposition metrics (F_{\max} , $AUI_{F>0.5}$ and DC_D as explanatory variables). These equations were used to identify critical current intensities beyond which detectable, moderate, and severe benthic impacts were not predicted to occur, including uncertainty. Two ranges of uncertainty in each critical current intensity threshold were calculated as (i) the regression models' 95% confidence intervals and (ii) the estimate that NewDEPOMOD predicts F_{\max} with an accuracy of $\pm 40\%$, based on a literature review of DEPOMOD's accuracy in previous studies (Relationships between site hydrodynamics and deposition section). The higher critical current intensity (i.e. the conservative value) of the two ranges was then selected.

The maximum deposition footprint [i.e. largest AUI (AUI_{\max}) and farthest DC (DC_{\max}) for each deposition rate] was compiled to summarize the worst possible impact for each farm type. A regular deposition rate vector (F_n) was built that ranged from the minimum detectable flow (0.5 kg $m^{-2} year^{-1}$, as mentioned) to the highest peak deposition (i.e. the maximum of the 54 values of F_{\max}). Corresponding vectors of the two metrics AUI_n and DC_n were provided for the 54 scenarios, and the largest values of AUI_n and DC_n for each type of farm were selected to build the upper boundary of the envelope curve.

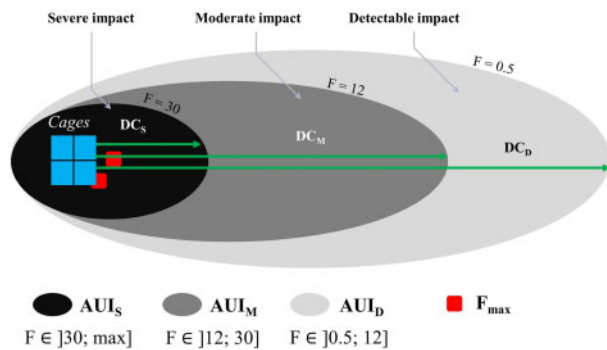


Figure 5. Diagram of a deposition footprint and the metrics used to describe it. Benthic impacts were classified according to three deposition ranges (F in kg solids $m^{-2} year^{-1}$) in detectable (D), moderate (M), or severe (S) impacts. DC_F (in m): maximum distance from cages at which deposition ranges can be detected; AUI_F (in m^2): area under farm influence for a deposition range; F_{\max} (in kg solids $m^{-2} year^{-1}$): maximum deposition rate in the grid.

Results

Suitable areas for fish farming in the NE Lagoon

In the coastal zone, 13.31 km^2 were suitable for Small farms, while 1.38 km^2 were suitable for Medium and Large farms. The off-coast zone covered 45.94 km^2 that were suitable for Medium and Large farms. The deep zone covered 23.63 km^2 that were suitable for Large farms. The total area suitable for each type of farm in the NE Lagoon was obtained from these values.

Contrasting site hydrodynamics in the NE Lagoon

The 36 sites selected in the NE Lagoon had contrasting hydrodynamic regimes (Figure 6 and Supplementary Table S1). To visualize this variability, we represented a tidal cycle averaged over the 15-day period from spring tide to neap tide of hourly barotropic current intensity using rose distributions of current for several of the sites. Most barotropic currents were oriented parallel to the coastline: northwest-southeast at most sites and north-south at sites between Grande-Terre and Petite-Terre (e.g. sites 10 and 11)

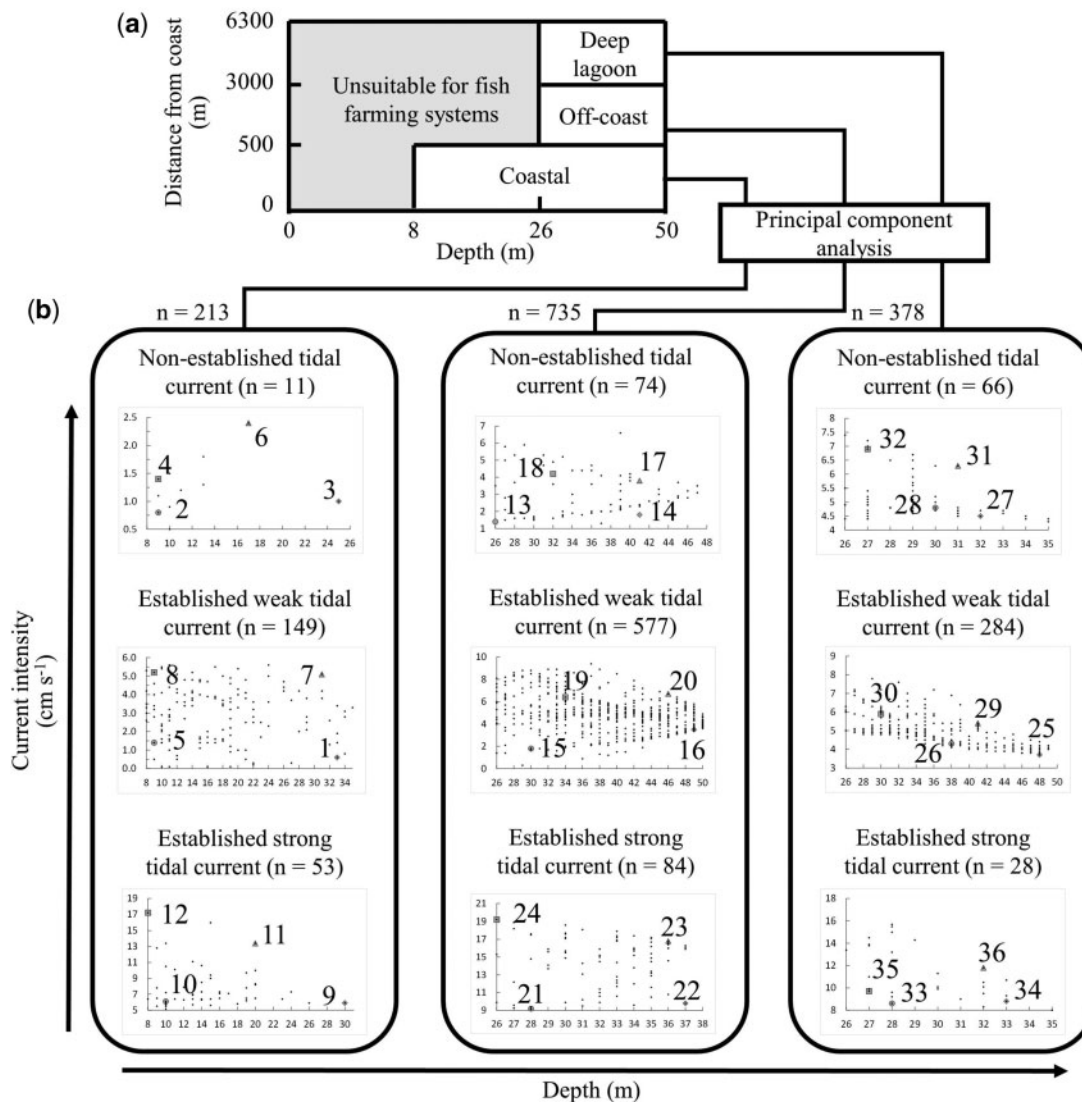


Figure 6. Process used to select sites with contrasting hydrodynamic regimes in Mayotte's North-East Lagoon: (a) definition of three aquaculture zones (group of sites) as a function of distance from the coast and depth criteria, and (b) site distribution plot (depth vs. current intensity) for each cluster built from the statistical analysis. Four sites with contrasting current intensities and depth were selected in each cluster: circle, low intensity/low depth; diamond, low intensity/high depth; square, high intensity/low depth; triangle, high intensity/high depth.

(Figure 7). Rose distributions with the most elliptical shapes (e.g. sites 4, 6, and 13) were associated mostly with low currents ($< 5 \text{ cm s}^{-1}$) and representative of non-established barotropic current (Figure 7). In contrast, sites with higher intensity currents had more established direction and thus the least elliptical shapes (Figure 7).

Feed- and faeces-settling results

Settling velocities

Faeces-settling velocities of all red drum size categories had a mean ($\pm 1 \text{ SD}$) of $0.64 \pm 0.39 \text{ cm s}^{-1}$ (Table 3) and differed significantly between all four fish size categories tested (Kruskal–Wallis test, $p < 0.001$). Faecal particles from small fish settled significantly faster than those of other size categories, but other pairwise comparisons showed no clear distinctions between

size categories (Table 3). Feed-settling velocity ranged from 3.67 to 15.68 cm s^{-1} and generally increased with pellet diameter (Table 4). Differences in settling velocities between all pellet categories were large and significant (Mann–Whitney U test, $p < 0.001$ for all pairwise comparisons).

Settling-velocity inputs for NewDEPOMOD

Pooled settling data for the four fish size categories and three pellet categories were compared to Gaussian and lognormal univariate distributions. Skewness (3.5) and kurtosis (26.4) coefficients estimated for faeces-settling data suggested an asymmetric, right-skewed, and heavy-tailed distribution of the samples compared to a normal distribution (which has skewness = 0 and kurtosis = 3). This was due to the large proportion of high settling velocities and the absence of negative values. In contrast, low skewness and

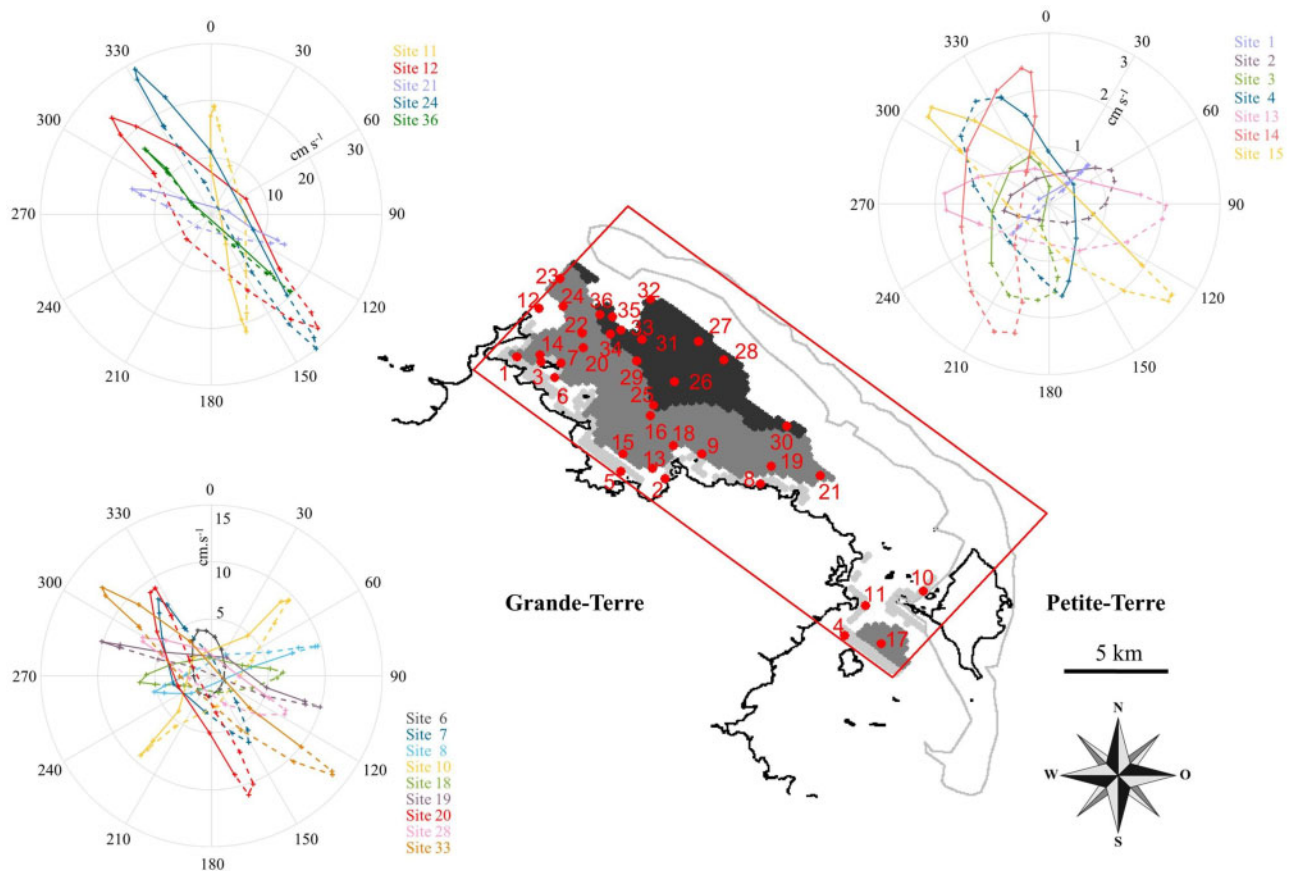


Figure 7. Aquaculture zones and sites in Mayotte’s North-East Lagoon. Zones were defined as a function of depth and distance from the coast as coastal (<500 m from the coast and ≤8 m deep: light grey), off-coast (500–3000 m from the coast and ≥26 m deep: medium grey), and deep lagoon (>3000 m from the coast and ≥26 m deep: dark grey). Twelve sites were selected in each zone (36 in total) to represent the range of hydrodynamic regimes in the area. The red rectangle indicates the domain modelled in the ROMS. Rose distribution plots of extracted hourly depth-averaged currents simulated by ROMS are shown for certain sites. In the roses, dashed and solid lines represent ebb and flow phases of the hourly depth-averaged current, respectively.

Table 3. Faecal particle-settling velocity (cm s^{-1}) of four red drum (*S. ocellatus*) commercial size categories (small: 648 g, medium: 1152 g, large: 1913 g, very large: 3155 g).

Fish category	Sample size (n)	Settling velocity (cm s^{-1})		
		Mean ± SD	Min	Max
Small	712	0.76 ± 0.39 ^a	0.27	5.24
Medium	712	0.60 ± 0.32 ^b	0.20	2.69
Large	712	0.66 ± 0.46 ^{bc}	0.17	4.04
Very large	712	0.57 ± 0.33 ^{cd}	0.21	4.33
All categories	2848	0.64 ± 0.39	0.17	5.24

The Mann–Whitney *U* test was used for pairwise comparison; different letters indicate differences significant at $p < 0.001$.

kurtosis values (0.0 and 2.5, respectively) obtained for feed-settling data indicated that feed particle-velocity distributions were more symmetric. Consequently, a lognormal (mean = 13.51, $SD = 2.10$) and Gaussian (mean = 0.64, $SD = 0.39$) distribution were set for the settling velocity of faeces and feed pellets, respectively. Note that distribution parameters (μ and σ^2 for log-normal, μ and σ for Gaussian) are estimated from these values directly in NewDEPOMOD.

Table 4. Measured settling velocities for red drum Nutrima® feed pellets as a function of diameter.

Pellet diameter (mm)	Sample size (n)	Settling velocity (cm s^{-1})	
		Mean	SD
1.2	31	3.67	0.65
2.2	31	7.40	0.58
3.2	31	9.84	0.75
4.5	31	11.26	0.89
6.0	31	13.60	1.19
9.0	31	15.67	1.12
Pooled 4.5/6.0/9.0	93	13.51	2.10
All diameters	186	10.24	4.05

Predicted waste deposition footprint

Deposition footprint results

Deposition footprints tended to have an elliptical shape and extend in the direction of local tide currents. Among the 54 scenarios, the model predicted the highest deposition rates directly beneath cages, which decreased as distance from the cages increased (Table 5; details in Supplementary Table S2). A scenario with a Large farm (Oco-L₂₄, off-coast zone, Large farm, site 24)

Table 5. Waste dispersion predicted for 54 scenarios with three types of red drum cage farms: Small (23 t of fish year⁻¹), Medium (299 t of fish year⁻¹), and Large (2079 t of fish year⁻¹) under contrasting hydrodynamic regimes in Mayotte's North-East Lagoon.

Metric	Unit	Small (n = 12)		Medium (n = 15)		Large (n = 27)	
		Min	Max	Min	Max	Min	Max
F_{\max}	kg m ⁻² year ⁻¹	1.2	10.7	5.8	44.0	4.8	27.0
Detectable impact							
F ∈ [0.5; 12]	% of scenarios		100		100		100
AUI _D	m ²	1500	4700	12 500	72 600	82 700	475 800
DC _D	m	20	90	100	740	110	850
Moderate impact							
F ∈ [12; 30]	% of scenarios		0		64		19
AUI _M	m ²	0	0	0	2600	0	29 500
DC _M	m	0	0	0	20	0	20
Severe impact							
F ∈ [30; max]	% of scenarios		0		14		0
AUI _S	m ²	0	0	0	1500	0	0
DC _S	m	0	0	0	10	0	0

F, deposition rate or range (in kg solids m⁻² year⁻¹); AUI_F, area under influence for a given F (in m²); DC_F, distance of influence from cages for a given F (in m). Dispersion metrics are given for three thresholds based on F found in the literature.

had the farthest DC_D, with a detectable impact up to 850 m. In 38 of 54 scenarios, particles released from cages were exported from the domain (i.e. >1000 m); thus, waste can be deposited even farther from the cages. Up to 21% of the particle mass released was exported from the domain; however, since deposition rates on domain edges were always below the detectable threshold, the scenario simulations effectively captured the area impacted by farm waste.

The type of farm strongly influenced the predicted deposition rate and area of seabed impacted. Farm types differed in production scale, but also in the number of cages, cage type, and cage layout (Figure 8). The highest deposition rate (44 kg m⁻² year⁻¹) was generated by a Medium farm (Co-M₁, coastal zone, site 1; Figure 8) and Medium farms always had higher F_{\max} than Large farms at a given site. For AUI, Large farms had the highest AUI_{F>0.5} (0.1–0.5 km²), covering up to 58 times the total cage area. Impacts of Small farms remained detectable, with a maximum F_{\max} of 10.7 kg m⁻² year⁻¹ at site 2 (Co-S₂) and an AUI_D that ranged from 1500 to 4700 m². Impacts of Medium farms were detectable (33% of the scenarios), moderate (54%) or severe (13%). AUI_M and AUI_S ranged from 200 to

2600 m² and 400 to 1500 m², respectively. No severe impact was predicted for Large farms, and moderate impact was predicted for 19% of the scenarios. AUI_M ranged from 3200 to 29 500 m². In the deep zone, impacts of Large farms remained detectable, with a maximum F_{\max} of 11.9 kg m⁻² year⁻¹ at site 28 (DI-L₂₈) and an AUI_D that ranged from 3200 to 29 500 m². When examining the largest AUI and farthest DC as a function of deposition rate among farms (Figure 9), the AUI was larger for Large farms than for Medium farms for F up to ca. 26 kg m⁻² year⁻¹; above this threshold, the AUI for Large farms decreased sharply.

Relationships between site hydrodynamics and deposition

Results of simple linear regression between current or depth and three deposition metrics (F_{\max} , AUI_{F>0.5}, and DC_D) are presented in the Supplementary Table S3. Mean barotropic current intensity was strongly and negatively correlated with F_{\max} and strongly and positively correlated with DC_D, at least for Medium and Large farms. These relationships indicated greater dilution of waste as current intensity increased. For instance, in Medium farm scenarios, F_{\max} was 82% lower at the site with the highest current intensity (site 24, 19.2 cm s⁻¹) than at the site with the lowest current intensity (site 1, 0.6 cm s⁻¹). In contrast, correlations between depth and F_{\max} , AUI_{F>0.5}, or DC_D were weak ($R^2 < 0.2$) and never significant ($p > 0.1$) for Small, Medium, and Large farms, indicating little influence of depth on deposition metrics. The influence of depth was notable mainly under low current intensities. For instance, in scenarios Co-S₁ and Co-S₂, in which current had a similar low intensity (<1 cm s⁻¹), Small farms had F_{\max} of 5.1 and 10.7 kg solids m⁻² year⁻¹ at a depth of 33 and 9 m, respectively.

Regressions between current and the deposition metrics yielded the following equations for mean barotropic current intensity (cm s⁻¹) as a function of F_{\max} (kg m⁻² y⁻¹): $\ln(y) = -0.290x + 2.466$ ($R^2 = 0.578$, $p < 0.05$), $-0.090x + 3.095$ ($R^2 = 0.906$, $p < 0.01$), and $-0.124x + 2.987$ ($R^2 = 0.805$, $p < 0.01$) for Small, Medium, and Large farms, respectively (Figure 10). Critical current intensities beyond which detectable, moderate, and severe benthic impacts were not predicted to occur varied

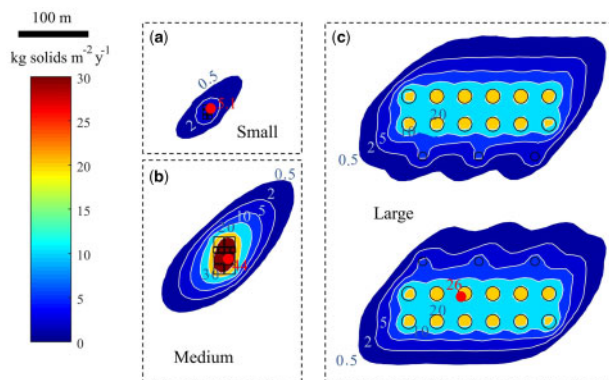


Figure 8. Deposition footprint at site 1 for a (a) Small farm, (b) Medium farm, and (c) Large farm. Black squares and circles represent cages. Red circles indicate the maximum deposition rate (F_{\max}).

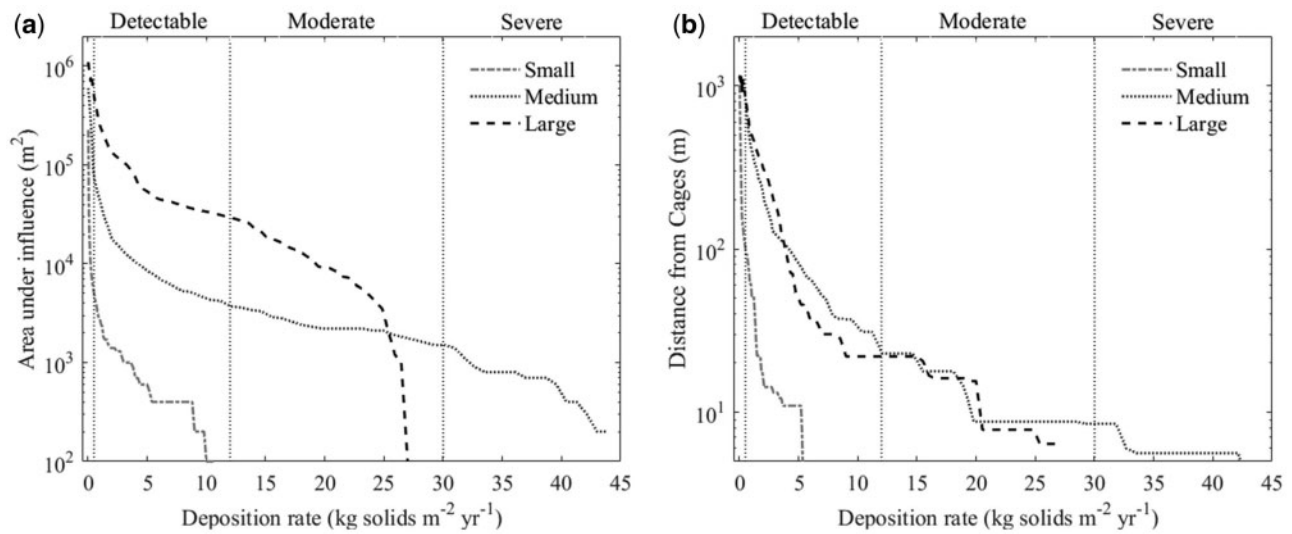


Figure 9. Maximum deposition footprints predicted for a variety of hydrodynamic regimes for Small ($n = 12$ regimes), Medium ($n = 15$), and Large ($n = 27$) farms as a function of deposition rate: (a) the largest area under influence and (b) the farthest distance from the cages that any particle was deposited. Vertical dotted lines indicate deposition thresholds for detectable, moderate, and severe impact.

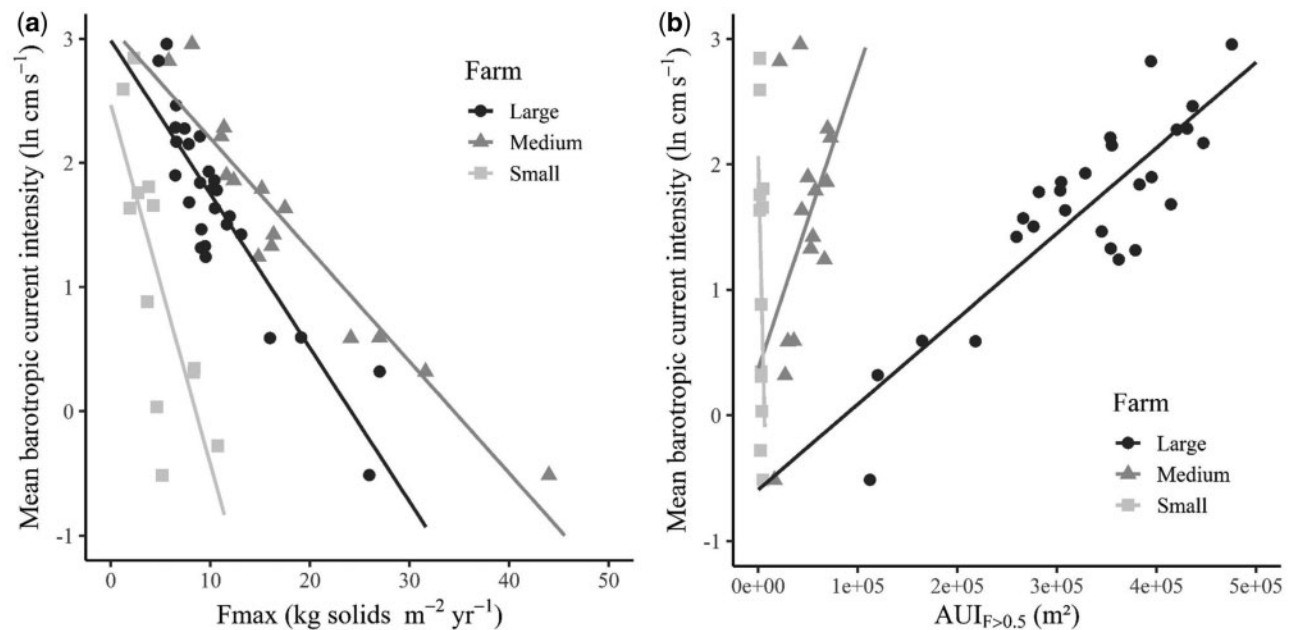


Figure 10. Linear regression between mean barotropic current intensity and (a) maximum solid deposition rate (F_{max}) and (b) total area under farm influence ($AUI_{F>0.5}$) predicted under various hydrodynamic regimes in Small ($n = 12$), Medium ($n = 15$), and Large farm ($n = 27$) scenarios. Current data were ln-transformed.

among farm types (Table 6). According to these current intensity thresholds and considering model (regression and NewDEPOMOD) uncertainties, moderate impact can be prevented in Medium and Large farms if mean current intensity exceeds 10.2 cm s^{-1} (9.9% of the area suitable for Medium farms in the NE Lagoon) and 6.8 cm s^{-1} (18.3% of the area suitable for Large farms), respectively. In contrast, to prevent detectable impact, mean currents of ca. $25\text{--}30 \text{ cm s}^{-1}$ would be required for all three farm types, but no sites in the NE Lagoon have this current

intensity. These critical limits of current intensity could be adapted for other deposition thresholds using the relationships between current intensity and maximum deposition rate provided in this study.

Discussion

Modelling limits and advantages

The present study used three different models to compare waste deposition footprints of different scenarios and to identify those

Table 6. Critical current intensity (CCI in cm s^{-1}) (conservative values that include uncertainty and, in parentheses, values estimated directly from regression models) required to reduce peak waste deposition rates (F_{max} in $\text{kg solids m}^{-2}\text{year}^{-1}$) above detectable (F_{D} in $\text{kg solids m}^{-2}\text{year}^{-1}$, with $F \in [0.5; 12]$), moderate (F_{M} , with $F \in [12; 30]$) severe (F_{S} , with $F \in [30; \text{max}]$) impact thresholds for Small, Medium, and Large farms.

Farm scenario	Characteristic	Benthic impact		
		($F_{\text{max}} < F_{\text{D}}$)	($F_{\text{max}} < F_{\text{M}}$)	($F_{\text{max}} < F_{\text{S}}$)
Small	CCI (cm s^{-1})	24.8 (10.2)	1.4 (0.4)	0.2 (0.0)
	A (km^2)	0	11.625	130.625
	A (%)	0	87.3	98.1
Medium	CCI (cm s^{-1})	29.8 (21.1)	10.2 (7.5)	3.2 (1.5)
	A (km^2)	0	4.688	39.500
	A (%)	0	9.9	83.5
Large	CCI (cm s^{-1})	24.9 (18.6)	6.8 (4.5)	1.4 (0.5)
	A (km^2)	0	13.000	70.438
	A (%)	0	18.3	99.3

The area (A) of the Mayotte North-East Lagoon with mean barotropic current intensity greater than or equal to each CCI was calculated for Small, Medium, and Large farm types in absolute value (km^2) and relative to the total area suitable per farm type (%).

that would minimize benthic impacts of aquaculture at the sub-lagoon scale. A hydrodynamic model was used to study the hydrodynamics in the study zone and extract current and depth data for 36 contrasting sites, a farm-scale model was used to estimate waste emissions from three farm types, and a waste dispersion model was used to simulate deposition footprints in 54 aquaculture scenarios. Limits and advantages related to the parametrization of each model, as well as their consequences on model outputs and potential application of the study's framework elsewhere are discussed below.

First, the hydrodynamic model (ROMS) used in this study considered the tide as the only forcing variable. Although tide is the main forcing variable in this system (De La Torre et al., 2008; Chevalier et al., 2015), it can vary spatially and temporally (seasonally or inter-annually) due to wind, swell, and intra-lagoon waves. These forcing variables may modify current intensity and/or direction locally at some sites. For instance, wind likely has a greater influence at shallow sites, due to greater impact of friction on the seabed, whereas swell increases water fluxes along the reef, pushing water out of reef openings and passages (Chevalier et al., 2015). Studying current variations at a finer scale, by including wind, swell, or wave forcing and their effects on waste deposition, could be a future course of research. Applying this study's framework to another region would require examining the specific characteristics of that region's hydrodynamics and probably the effects of these forcing variables.

In this study, NewDEPOMOD was applied for the first time to red drum farming, which required adapting only species-specific parameters (Cromey et al., 2009), such as particle-settling velocities, feed digestibility, and feed and faeces composition. In this study, we used the FINS farm-scale model, which use red-drum specific digestibility data and red drum feed composition data, to provide realistic and detailed time series predictions of waste fluxes under routine farming conditions. The advantage of using a farm-scale model such as FINS to do so, rather than using NewDEPOMOD alone, is that waste emissions can vary at the

cage scale as a function of daily stocked biomass and feeding practices instead of remaining constant over time. Providing detailed rearing input data to DEPOMOD has been shown to increase its accuracy (Cromey et al., 2012; Chang et al., 2014). We thus believe that combining FINS and NewDEPOMOD may increase the accuracy of NewDEPOMOD predictions. In this study, new faeces and feed-particle settling data for the commercial feeds used by farms (and parametrized in FINS) were acquired. They may also help increase the accuracy of the predicted deposition rates and decrease parameter uncertainties in NewDEPOMOD.

We examined effects of differing hydrodynamics on deposition footprints but did not consider other important highly site-specific processes, such as particle resuspension and effects of wild fish, which can also influence results greatly. Resuspension can pick up previously settled particles and redistribute them over larger areas, thus decreasing organic-matter accumulation and its ecological effects near cages (Keeley et al., 2013; Broch et al., 2017). A seabed's sensitivity to resuspension depends greatly on substrate type and texture (Law et al., 2016; Carvajalino-Fernández et al., 2020a), as well as vertical structure, disturbance history and, for sediment substrates, resident biota (Sanford, 2008). Dispersion models with spatially explicit sediment resuspension parameters have been found to be more accurate than those with constant default resuspension parameters or those that ignore resuspension (Carvajalino-Fernández et al., 2020b). Substrate characteristics can vary greatly at the sub-lagoon scale and were not examined in this study; therefore, we did not intend to set specific parameters for each site. In previous studies, wild fish have shown a potential to reduce the amount of organic matter deposited on the seabed by 14% in some farms (Ballester-Moltó et al., 2017) by scavenging uneaten feed and, to a lesser extent, fish faeces (Fernandez-Jover et al., 2008). The magnitude of particulate removal by wild fish can vary, however, according to the biomass and species composition of their assemblages (Dempster et al., 2005), which also depends on site distance from the coast and farm scale (Dempster et al., 2002). Thus, because the wild fish effect also likely varies at the sub-lagoon scale, it was not simulated. The absence of resuspension and wild fish effects probably resulted in overprediction of deposition rates, particularly near the cages, where most uneaten feed settles. Model outputs should thus be considered as primary footprints and conservative worst-case deposition rates.

We used NewDEPOMOD in a new environmental context without validating it, since this study analysed exploratory scenarios with hypothetical farms. Model validation is an integral part of the modelling process that improves understanding of a model's error, overall accuracy, and spatial applicability. The accuracy of DEPOMOD and some of its derived models (CODMOD, MACAROMOD) has been assessed for a variety of hydrodynamic conditions, including both depositional and highly dispersive sites. Differences between observations and DEPOMOD predictions of waste deposition for salmon farms in Scotland with low-to-medium mean current intensity (3.6–6.9 cm s^{-1} , depending on the layer) ranged from 13 to 20%, depending on the site (Cromey et al., 2002). In a seabass and seabream farm at a site with low mean current intensity (1.3–2.2 cm s^{-1}) in the eastern Mediterranean, MERAMOD (Cromey et al., 2012) had a mean accuracy of 44% (with optimized parameters), with more accurate predictions in high-flux zones ($\pm 35\%$) than in low-flux zones ($\pm 111\%$). More recently, MACAROMOD was validated for four farms in the northeastern Atlantic that produced seabass,

seabream, and meagre. Its accuracy ranged from 12 to 34% [calculated from Figure 5 in Riera *et al.* (2017)] at three sites with medium-to-high mean current intensity (8–25 cm s⁻¹) but was lower ($\pm 94\%$) at the fourth site (6 cm s⁻¹). Other studies of salmon farms in Canada (Chamberlain and Stucchi, 2007) and New Zealand (Keeley *et al.*, 2013) reported similar patterns between observed and predicted footprints for optimized models, but model accuracy was not estimated or reported. This demonstrated that DEPOMOD's transport equations are generally transferable to different hydrodynamic environments, including the conditions tested in this study, as long as good input data are provided and models are optimized. Most studies optimized model accuracy by deactivating DEPOMOD's resuspension module (Chamberlain and Stucchi, 2007; Cromey *et al.*, 2012; Keeley *et al.*, 2013; Chang *et al.*, 2014), except for one (Cromey *et al.*, 2009), which opens a debate on the quality of the models and parameters used to represent resuspension. The main changes made to NewDEPOMOD compared to DEPOMOD concern the modelling of resuspension and seabed processes (Black *et al.*, 2016; SAMS, 2020). Since resuspension was not simulated in this study, we expect NewDEPOMOD's accuracy in our scenarios to be similar to that of the original model. In future research, it would be necessary to examine NewDEPOMOD's accuracy for real and operating farms in Mayotte Lagoon.

Variability in impact across hydrodynamic regimes and farm characteristics

Systematic exploration of multiple aquaculture scenarios had the main advantage of allowing quantitative relationships between site hydrodynamics and deposition footprint metrics to be estimated. The physical properties of depth and current intensity are often presented as equally desirable attributes promoting dispersion (Hargrave, 2002; Belle and Nash, 2008). In this study, depth did not influence waste dispersion significantly, while a significant decrease in solid accumulation near the cages and a broader deposition footprint were observed as current intensity increased. The lack of a significant influence of depth may be explained in part by the narrower range of depths in the scenarios (factor of 6 between minimum and maximum values) than of current intensities (factor of 30). A previous large study that evaluated environmental impacts of finfish and shellfish aquaculture across Europe (Borja *et al.*, 2009) found that mean current intensity had a much larger influence than depth in reducing biotic index values. In our study, the significant relationships between current intensity and three deposition metrics (F_{\max} , $AUI_{F>0.5}$, and DC_D) allowed the use of current intensity to predict waste-particle deposition. The relationship between mean barotropic current intensity and maximum deposition rate (F_{\max}) decreased logarithmically, which indicated that a small increase in current intensity can provide a large dilution effect.

The amount of fish waste produced and released into the environment is related to the total fish biomass in stock; however, our results showed no correlation between maximum deposition rates and farm scale, and a strong influence of the farm layout. When simulated under identical hydrodynamic regimes, scenarios with Medium farms always had higher maximum deposition rates F_{\max} (over small benthic areas) than Large farms. Since the Large farm releases much more waste per day than the Medium farm, this difference is probably due to cage density and layout (Figure 8). Indeed, Small and Medium farms have interdependent

cages to reduce installation costs and the number of mooring lines (Cardia and Lovatelli, 2015). This interdependence reduced cage spacing (ca. 3 m vs. 20 m on Large farms), thus concentrating waste emission on a smaller area, which logically increased maximum waste deposition on the seabed locally. Aquaculture management guidelines generally recommend a “minimum farm distance” to avoid cumulative effects of multiple farms (Cardia *et al.*, 2017). Based on this principle, “minimum cage spacing” could be added to reduce the risk of high waste accumulation on the seabed. These results demonstrate that farm scale is not the main factor that influences deposition rate; instead, management of the entire farm (e.g. cage position, cage spacing) must be considered to predict impacts accurately, as also highlighted in a recent paper (Burić *et al.*, 2020).

Interpreting the deposition footprint

The impact metrics used may influence the interpretation of impact. The need to manage waste in intensive fish farming has led to a debate that opposes the approaches of concentrating waste over a small area vs. diluting and dispersing it to avoid excessive accumulation near the cages (Keeley *et al.*, 2019). Depending on the approach, different metrics can be used to characterize the waste dispersion footprint and the degree of impact. Some may consider maximum deposition rate (regardless of the area impacted or distance of impact) as the most important metric, while others may consider the maximum distance (and thus area) of deposition (regardless the intensity of the flux) as the most important. Ideally, both metrics should be considered, since they can influence interpretation of potential impact on the seabed. For maximum deposition rate, Medium farms would have the highest impacts, since they always had the highest deposition rates, while for maximum distance, Large farms would have larger impacts than Medium farms, since their total AUI was always larger (4.4–18.4 times). However, reasoning in terms of “maximum” has no sense if the flux considered is not likely to cause any impact. This is why it is crucial to identify relationships between deposition rates and ecological responses as well as ecological thresholds beyond which significant change in ecosystem state and quality can occur (Groffman *et al.*, 2006). These relationships are highly specific to a given ecosystem (Keeley *et al.*, 2013) and have been developed and implemented mainly in temperate environments, while tropical environments have received little attention. For instance, a biotic index such as the multivariate AZTI Marine Biotic Index (M-AMBI), widely used to characterize the ecological status of benthos in temperate environments, has not yet been adapted or validated for tropical ecosystems or species. This is also true for tools that assess carrying capacity in general (Aubert *et al.*, 2020). Therefore, we suggest below a possible interpretation and application of this study based on literature thresholds.

Based on ecological and regulatory thresholds from the literature, most predicted impacts of red drum fish farming in Mayotte's NE Lagoon were located near farms. In ca. 70% of the scenarios, detectable impacts were predicted up to 500 m from the farm. In the most dispersive sites, they were predicted up to 850 m from the farm (Figure 9b and Supplementary Table S2), and traces of waste did disperse farther. In the literature, traces of fish waste have also been recorded 500–1000 m from a farm (Broch *et al.*, 2017; White *et al.*, 2017; Woodcock *et al.*, 2018; Keeley *et al.*, 2019) and even farther (Bannister *et al.*, 2016).

Thus, a safe distance of ca. 1000 m between sites seems necessary to avoid cumulative effects of multiple farms and to protect zones of ecological interest from fish farm waste. In the range of hydrodynamic regimes tested, moderate and severe impacts were found up to 20 and 10 m from the cages, respectively. This result is in line with results of a meta-analysis of 70 aquaculture studies from around the world that estimated that the distance at which environmental impact is extremely unlikely (the “farm ecotone”) is 90 m (Froehlich *et al.*, 2017). In the AZE framework, specific EQS (and thus impacts) are generally allowed up to 25–50 m around cages in EU countries (Katavić *et al.*, 2005; GFCM, 2012) and up to 200 m in other regions (e.g. United States, Australia, or New Zealand) (Wang *et al.*, 2020). Based on these regulatory distances, moderate and severe impacts, if they occur, would remain in the AZE for all three farm types. If acceptable impact distances (AZE limits) and/or deposition rate thresholds used to define moderate or severe impacts change, these conclusions could change. For this reason, we plotted the maximum distance and maximum area impacted as a function of deposition rate (Figure 9). One can use these plots to adapt the conclusions to other ecological or regulatory thresholds. For instance, for a maximum EQS of 20 kg solids $\text{m}^{-2}\text{year}^{-1}$ allowed within 50 m of the cages, some of the Medium and Large farm scenarios would have unacceptable impacts. Compared to a series of maps, this type of plot provides an easy-to-understand summary of possible benthic impacts of multiple farming scenarios in a given zone.

The areas in the NE Lagoon where hydrodynamic regimes could reduce benthic impacts below detectable, moderate, and severe impacts were examined for the three farming scenarios. The model's results suggest that a low mean current intensity (3.2 cm s^{-1}) could prevent severe impacts of Medium farms. Based on this hypothesis, most of the area (83.5%) suitable for this farm type in the NE Lagoon would have sufficiently high current intensity to prevent such impact. Since severe impacts were predicted only for Medium farms, they should be unlikely to occur in the NE Lagoon. Based on the current limits, we can also hypothesize that moderate impacts on Medium and Large farms can be avoided only in limited areas: 9.9 and 18.3% of the area suitable for Medium and Large farms, respectively. Expecting zero impact is unrealistic, in any case, since very intense currents ($25\text{--}30\text{ cm s}^{-1}$) are necessary to prevent detectable impacts from the three farm types, and the maximum mean current intensity in the NE Lagoon was ca. 20 cm s^{-1} . Furthermore, such a high current intensity may reduce fish growth potential (Plaut, 2001), increase feed conversion ratio (Ferreira *et al.*, 2012), and deform nets enough to endanger fish (GESAMP, 2001; Cardia *et al.*, 2017). Similar ranges of current intensity were proposed for salmon culture in Scotland as a function of biomass stock: $0\text{--}5\text{ cm s}^{-1}$ for $0\text{--}499\text{ t}$ of biomass, $5\text{--}10\text{ cm s}^{-1}$ for $499\text{--}999\text{ t}$ and $>10\text{ cm s}^{-1}$ for $>1000\text{ t}$ (Cardia *et al.*, 2017). Another classification of site sensitivity to fish farming based on current intensity was proposed in Norway: <3 , $4\text{--}6$, $7\text{--}10$, and $11\text{--}25\text{ cm s}^{-1}$ for very sensitive, moderately sensitive, slightly sensitive, and not sensitive, respectively (Velvin, 1999). This type of environmental recommendation should be considered at the same time as other biophysical requirements for farmed species and systems to ensure technically feasible and environmentally sustainable development of aquaculture.

Conclusion and perspectives

The present study proposed a generic five-step analysis framework to facilitate zoning and site selection based on predicting

the deposition footprint in a broad range of explorative scenarios and applied to a case study of red drum farming in Mayotte. Legislation for fish farm licensing in countries such as France, and thus Mayotte, requires that environmental impact assessment be performed as a function of the amount of farm production expected. Our results indicate that this approach may be overly simplistic and that current intensity and cage layout are other important factors to consider. The combined use of hydrodynamic models, farm-scale models, and particle-dispersion models can consider many farm and site-specific factors that can influence benthic impact. Using such tools in the licensing process of new farms in France, as done in Canada and Scotland (Hills *et al.*, 2005), would address potential impacts of aquaculture in a meaningful way. In the meantime, by using them for exploratory analysis at a large scale, we provided useful information to facilitate aquaculture zoning, site selection, and management. Worst-case impacts (i.e. maximum distance and area for a given deposition rate) were provided for multiple farm types. Practical recommendations for cage and farm spacing to reduce the concentration of farm waste on the seabed were also provided. Finally, critical current intensities were provided to provide information about the dispersive potential of sites in the NE Lagoon of Mayotte. These critical current intensities and the hydrodynamic-based site clustering method used in this study could be used to build spatial layers of environmentally suitable zones. Incorporating them in spatial analysis (e.g. GIS) and overlaying them with other physical, chemical, biological, and social attributes would provide a comprehensive multi-criteria assessment and create maps that could identify potential sites and help achieve successful marine plans more easily (Stelzenmüller *et al.*, 2017). In the future, other near-field and far-field effects of fish farming in Mayotte Lagoon should also be examined. Given the abundance of coral reefs in the lagoon and their potential sensitivity to water nutrient enrichment (D'Angelo and Wiedenmann, 2014), we recommend studying in priority the effects of dissolved nutrient emissions from fish farming on coral reef ecosystems.

Supplementary data

Supplementary material is available at the ICESJMS online version of the manuscript.

Funding

This study was performed as a part of a PhD thesis in the CAPAMAYOTTE project, Phase 2 (2015–2018), funded by the Natural Marine Park of Mayotte and the Mayotte County Council.

Acknowledgements

The authors gratefully acknowledge Cristele Chevalier for providing access to predictions of the ROMS model. We thank J.C. Falguière and S. Devillers for helping to perform the settling experiment. We thank Dr M.S. Corson for careful revision of the English. We thank R. Weeks and T. Adams for their support in using NewDEPOMOD. Finally, we thank the two anonymous reviewers for their valuable suggestions and comments.

Authors' contributions

KC: conceptualization, drafting, experiments, analysis, design, and methodology; MC: conceptualization, experiments, and revision; DC: experiments and revision; JA: revision; JS: experiments

and revision; AF: conceptualization, design, methodology, analysis, and revision.

Data availability

The data underlying this article will be shared on reasonable request to the corresponding author.

References

- Aguilar-Manjarrez, J., Soto, D., and Brummett, R. 2017. Aquaculture zoning, site selection and area management under the ecosystem approach to aquaculture. Report ACS113536. Rome, FAO, and World Bank Group, Washington, DC, 395 pp. <http://www.fao.org/documents/card/en/c/4c777b3a-6afc-4475-bfc2-a51646471b0d/> (last accessed 30 December 2020).
- Aquapark. 2015. AquaPark Project Final eReport—planning and management of aquaculture parks for sustainable development of cage farms in the Philippines (AQUAPARK). 124 pp. https://www.academia.edu/7666623/Planning_and_management_of_aquaculture_parks_for_sustainable_development_of_cage_farms_in_the_Philippines (last accessed 30 December 2020).
- Aubert, A., Aschenbroich, A., Gaertner, J. C., Latchere, O., Archambault, P., and Gaertner Mazouni, N. 2020. Assessment of carrying capacity for bivalve mariculture in subtropical and tropical regions: the need for tailored management tools and guidelines. *Reviews in Aquaculture*, 12: 1–15.
- Ballester-Moltó, M., Sanchez-Jerez, P., and Aguado-Giménez, F. 2017. Consumption of particulate wastes derived from cage fish farming by aggregated wild fish. An experimental approach. *Marine Environmental Research*, 130: 166–173.
- Bannister, R. J., Johnsen, I. A., Hansen, P. K., Kutti, T., and Asplin, L. 2016. Near- and far-field dispersal modelling of organic waste from Atlantic salmon aquaculture in fjord systems. *ICES Journal of Marine Science*, 73: 2408–2419.
- Belle, S. M., and Nash, C. E. 2008. Better management practices for net-pen aquaculture. *In* *Environmental Best Management Practices for Aquaculture*, pp. 261–330. Ed. by C. S. Tucker and J. A. Hargreaves. Wiley-Blackwell, Oxford, UK.
- Black, K. D., Carpenter, T., Berkeley, A., Black, K., and Amos, C. 2016. Refining sea-bed process models for aquaculture. *New DEPOMOD Final Report*. Oban. 200 pp.
- Borja, Á., Rodríguez, J. G., Black, K., Bodoy, A., Emblow, C., Fernandes, T. F., Forte, J., *et al.* 2009. Assessing the suitability of a range of benthic indices in the evaluation of environmental impact of fin and shellfish aquaculture located in sites across Europe. *Aquaculture*, 293: 231–240.
- Börjeson, L., Höjer, M., Dreborg, K.-H., Ekvall, T., and Finnveden, G. 2006. Scenario types and techniques: towards a user's guide. *Futures*, 38: 723–739.
- Bostock, J., McAndrew, B., Richards, R., Jauncey, K., Telfer, T., Lorenzen, K., Little, D., *et al.* 2010. Aquaculture: global status and trends. *Philosophical Transactions of the Royal Society B: Biological Sciences*, 365: 2897–2912.
- Brigolin, D., Pastres, R., Nickell, T. D., Cromey, C. J., Aguilera, D. R., and Regnier, P. 2009. Modelling the impact of aquaculture on early diagenetic processes in sea loch sediments. *Marine Ecology Progress Series*, 388: 63–80.
- Brigolin, D., Porporato, E. M. D., Prioli, G., and Pastres, R. 2017. Making space for shellfish farming along the Adriatic coast. *ICES Journal of Marine Science*, 74: 1540–1551.
- Broch, O. J., Daae, R. L., Ellingsen, I. H., Nepstad, R., Bendiksen, E. A., Reed, J. L., and Senneset, G. 2017. Spatiotemporal dispersal and deposition of fish farm wastes: a model study from central Norway. *Frontiers in Marine Science*, 4: 1–15.
- Burić, M., Bavčević, L., Grgurić, S., Vresnik, F., and Krizan, J., Antonić, O. 2020. Modelling the environmental footprint of sea bream cage aquaculture in relation to spatial stocking design. *Journal of Environmental Management*, 270: 13 pages.
- Byron, C. J., Costa-Pierce, B. A. 2013. Carrying capacity tools for use in the implementation of an ecosystems approach to aquaculture. *In* *Site Selection and Carrying Capacity for Inland and Coastal Aquaculture*, pp. 87–101. Ed. by L. G. Ross, T. C. Telfer, L. Falconer, D. Soto, and J. Aguilar-Manjarrez. FAO/Institute of Aquaculture, University of Stirling, Expert Workshop, 6–8 December 2010. Stirling, UK. FAO Fisheries and Aquaculture Proceedings No. 21, Rome.
- Cardia, F., Ciattaglia, A., and Corner, R. A. 2017. Guidelines and criteria on technical and environmental aspects of cage aquaculture site selection in the Kingdom of Saudi Arabia. Food and Agriculture Organization of the United Nations and the Ministry of Environment, Water and Agriculture in the Kingdom of Saudi Arabia, Rome, Italy. 58 pp. <http://www.fao.org/publications/card/en/c/923513b9-83fa-423a-a1ee-904531205d35> (last accessed 30 December 2020).
- Cardia, F., and Lovatelli, A. 2015. *Aquaculture Operations in Floating HDPE Cages: A Field Handbook*. FAO and Ministry of Agriculture of the kingdom of Saudi Arabia, Rome. 152 pp.
- Carvajalino-Fernández, M. A., Keeley, N. B., Fer, I., Law, B. A., and Bannister, R. J. 2020a. Effect of substrate type and pellet age on the resuspension of Atlantic salmon faecal material. *Aquaculture Environment Interactions*, 12: 117–129.
- Carvajalino-Fernández, M. A., Søvik, P. N., Johnsen, I. A., Albretsen, J., and Keeley, N. B. 2020b. Simulating particle organic matter dispersal beneath Atlantic salmon fish farms using different resuspension approaches. *Marine Pollution Bulletin*, 161: 111685.
- Chamberlain, J., and Stucchi, D. 2007. Simulating the effects of parameter uncertainty on waste model predictions of marine finfish aquaculture. *Aquaculture*, 272: 296–311.
- Chang, B. D., Page, F. H., Losier, R. J., and McCurdy, E. P. 2014. Organic enrichment at salmon farms in the Bay of Fundy, Canada: DEPOMOD predictions versus observed sediment sulfide concentrations. *Aquaculture Environment Interactions*, 5: 185–208.
- Chary, K., Fiandrino, A., Covès, D., Aubin, J., Falguière, J. C., and Callier, M. D. 2019. Modeling sea cage outputs for data-scarce areas: application to red drum (*Sciaenops ocellatus*) aquaculture in Mayotte, Indian Ocean. *Aquaculture International*, 27: 625–646.
- Chevalier, C., Devenon, J.-L., Rougier, G., and Blanchot, J. 2015. Hydrodynamics of the Toliara Reef Lagoon (Madagascar): example of a Lagoon influenced by waves and tides. *Journal of Coastal Research*, 316: 1403–1416.
- Chevalier, C., Devenon, J. L., Pagano, M., Rougier, G., Blanchot, J., and Arfi, R. 2017. The atypical hydrodynamics of the Mayotte Lagoon (Indian Ocean): effects on water age and potential impact on plankton productivity. *Estuarine, Coastal and Shelf Science*, 196: 182–197.
- Corner, R. A., Brooker, A. J., Telfer, T. C., and Ross, L. G. 2006. A fully integrated GIS-based model of particulate waste distribution from marine fish-cage sites. *Aquaculture*, 258: 299–311.
- Cromey, C. J., Nickell, T. D., and Black, K. D. 2002. DEPOMOD—modelling the deposition and biological effects of waste solids from marine cage farms. *Aquaculture*, 214: 211–239.
- Cromey, C. J., Nickell, T. D., Treasurer, J., Black, K. D., and Inall, M. 2009. Modelling the impact of cod (*Gadus morhua* L.) farming in the marine environment-CODMOD. *Aquaculture*, 289: 42–53.
- Cromey, C. J., Thetmeyer, H., Lampadariou, N., Black, K. D., Kögeler, J., and Karakassis, I. 2012. MERAMOD: predicting the deposition and benthic impact of aquaculture in the eastern Mediterranean Sea. *Aquaculture Environment Interactions*, 2: 157–176.
- D'Angelo, C., and Wiedenmann, J. 2014. Impacts of nutrient enrichment on coral reefs: new perspectives and implications for coastal management and reef survival. *Current Opinion in Environmental Sustainability*, 7: 82–93.

- De La Torre, Y., Delattre, M., Idier, D., and Romieu, E. 2008. Modélisation courantologique du lagon de Mayotte. Rapport BRGM/RP-56334-FR. 133 pp.
- Dempster, T., Fernandez-Jover, D., Sanchez-Jerez, P., Tuya, F., Bayle-Sempere, J., Boyra, A., and Haroun, R. 2005. Vertical variability of wild fish assemblages around sea-cage fish farms: implications for management. *Marine Ecology Progress Series*, 304: 15–29.
- Dempster, T., Sanchez-Jerez, P., Bayle-Sempere, J., Giménez-Casalduero, F., and Valle, C. 2002. Attraction of wild fish to sea-cage fish farms in the south-western Mediterranean Sea: spatial and short-term temporal variability. *Marine Ecology Progress Series*, 242: 237–252.
- Dinhut, V., Nicet, J.-B., and Quod, J.-P. 2008. Suivi et état de santé 2007 des récifs coralliens de Mayotte. *Revue d'écologie (La Terre et la Vie)*, 63: 103–114.
- FAO. 2018. The State of World Fisheries and Aquaculture 2018—meeting the sustainable development goals. Licence: CC by-NC-SA 3.0 IGO. FAO, Rome. 227 pp. <http://www.fao.org/publications/card/en/c/I9540EN> (last accessed 30 December 2020).
- Fernandes, E., Ackefors, E., Sanchez-Mata, Scanlon, White., et al. 2001. The scientific principles underlying the monitoring of the environmental impacts of aquaculture. *Journal of Applied Ichthyology*, 17: 181–193.
- Fernandez-Jover, D., Sanchez-Jerez, P., Bayle-Sempere, J. T., Valle, C., and Dempster, T. 2008. Seasonal patterns and diets of wild fish assemblages associated with Mediterranean coastal fish farms. *ICES Journal of Marine Science*, 65: 1153–1160.
- Ferreira, J. G., Saurel, C., and Ferreira, J. M. 2012. Cultivation of gilt-head bream in monoculture and integrated multi-trophic aquaculture. Analysis of production and environmental effects by means of the FARM model. *Aquaculture*, 358–359: 23–34.
- Froehlich, H. E., Smith, A., Gentry, R. R., and Halpern, B. S. 2017. Offshore aquaculture: I know it when I see it. *Frontiers in Marine Science*, 4: 1–9.
- Gentry, R. R., Froehlich, H. E., Grimm, D., Kareiva, P., Parke, M., Rust, M., Gaines, S. D., et al. 2017b. Mapping the global potential for marine aquaculture. *Nature Ecology & Evolution*, 1: 1317–1324.
- Gentry, R. R., Lester, S. E., Kappel, C. V., White, C., Bell, T. W., Stevens, J., and Gaines, S. D. 2017a. Offshore aquaculture: spatial planning principles for sustainable development. *Ecology and Evolution*, 7: 733–743.
- GESAMP. 2001. Planning and Management for Sustainable Coastal Aquaculture Development. GESAMP reports and studies No. 68. Rome. 113 pp.
- GFCM. 2012. Report of the WGSC—ShoCMed Workshop on the definition and environmental monitoring within Allowable Zone of Effect (AZE) of aquaculture activities within the Mediterranean countries. Rome. 24 pp.
- Giles, H. 2008. Using Bayesian networks to examine consistent trends in fish farm benthic impact studies. *Aquaculture*, 274: 181–195.
- Gillibrand, P. A., and Turrell, W. R. 1997. Simulating the dispersion and settling of particulate material and associated substances from salmon farms. Aberdeen. 21 pp. https://www.researchgate.net/publication/320662425_Simulating_the_dispersion_and_settling_of_particulate_material_and_associated_substances_from_salmon_farms (last accessed 30 December 2020).
- Groffman, P. M., Baron, J. S., Blett, T., Gold, A. J., Goodman, I., Gunderson, L. H., Levinson, B. M., et al. 2006. Ecological thresholds: the key to successful environmental management or an important concept with no practical application? *Ecosystems*, 9: 1–13.
- Hadley, S., Macleod, C., and Ross, D. J. 2017. Implementation of NewDEPOMOD for Modelling the Depositional Footprint from Salmon Aquaculture in Storm Bay. Hobart, Tasmania. 13 pp.
- Hargrave, B. T. 1994. A benthic enrichment index. In *Modeling benthic impacts of organic enrichment from marine aquaculture*. Canadian Technical Report of Fisheries and Aquatic Sciences, 1949: 79–91.
- Hargrave, B. T. 2002. A traffic light decision system for marine finfish aquaculture siting. *Ocean and Coastal Management*, 45: 215–235.
- Hills, A., Spurway, J., Brown, S., and Cromey, C. 2005. Regulation and monitoring of marine cage fish farming in Scotland—Annex H—methods for modelling in-feed anti-parasitics and benthic effects. Stirling, 1–140. <https://www.sepa.org.uk/media/113511/fish-farm-manual-annex-h.pdf> (last accessed 30 December 2020).
- Holmer, M. 2010. Environmental issues of fish farming in offshore waters: perspectives, concerns and research needs. *Aquaculture Environment Interactions*, 1: 57–70.
- Jeanson, M., Anthony, E. J., Dolique, F., and Aubry, A. 2013. Wave characteristics and morphological variations of pocket beaches in a coral reef-lagoon setting, Mayotte Island, Indian Ocean. *Geomorphology*, 182: 190–209.
- Jusup, M., Klanjšček, J., Petricioli, D., and Legović, T. 2009. Predicting aquaculture-derived benthic organic enrichment: model validation. *Ecological Modelling*, 220: 2407–2414.
- Kapetsky, J. M., Aguilar-Manjarrez, J., and Jenness, J. 2013. A global assessment of offshore mariculture potential from a spatial perspective. FAO fisheries and aquaculture technical paper 549. 2013. 202 pp.
- Karakassis, I. 2013. Environmental interactions and initiatives on site selection and carrying capacity estimation for fish farming in the Mediterranean. In *Site Selection and Carrying Capacities for Inland and Coastal Aquaculture*, pp. 161–170. Ed. by L.G. Ross, T.C. Telfer, L. Falconer, D. Soto & J. Aguilar-Manjarrez. FAO/Institute of Aquaculture, University of Stirling, Expert Workshop, 6–8 December 2010. p. 282. Rome. <http://www.fao.org/tempref/FI/CDrom/P21/root/09.pdf> (last accessed 30 December 2020).
- Katavić, I., Herstad, T.-J., Kryvi, H., White, P., Franičević, V., and Skakelja, N. 2005. Guidelines to marine aquaculture planning, integration and monitoring in Croatia. Project “Coastal zone management plan for Croatia”. Zagreb. 78 pp. http://ccrm.vims.edu/publications/pubs/aquaculture_guidelines.pdf (last accessed 30 December 2020).
- Keeley, N., Valdemarsen, T., Woodcock, S., Holmer, M., Husa, V., and Bannister, R. 2019. Resilience of dynamic coastal benthic ecosystems in response to large-scale finfish farming. *Aquaculture Environment Interactions*, 11: 161–179.
- Keeley, N. B., Cromey, C. J., Goodwin, E. O., Gibbs, M. T., and Macleod, C. M. 2013. Predictive depositional modelling (DEPOMOD) of the interactive effect of current flow and resuspension on ecological impacts beneath salmon farms. *Aquaculture Environment Interactions*, 3: 275–291.
- Law, B. A., Hill, P. S., Milligan, T. G., and Zions, V. 2016. Erodibility of aquaculture waste from different bottom substrates. *Aquaculture Environment Interactions*, 8: 575–584.
- Le, S., Josse, J., and Husson, F. 2008. FactoMineR: an R package for multivariate analysis. *Journal of Statistical Software*, 25: 1–18.
- Lee, S., Hartstein, N. D., Wong, K. Y., and Jeffs, A. 2016. Assessment of the production and dispersal of faecal waste from the sea-cage aquaculture of spiny lobsters. *Aquaculture Research*, 47: 1569–1583.
- Lovatelli, A., Aguilar-Manjarrez, J., and Soto, D. 2013. Expanding mariculture farther offshore - technical, environmental, spatial and governance challenges, FAO Technical Workshop, 22-25, March 2010, Orbetello, Italy. In *FAO Fisheries and Aquaculture Proceedings No. 24*, p. 73. Ed. by FAO. Rome. www.fao.org/docrep/018/i3092e/i3092e00.htm (last accessed 30 December 2020).
- Magill, S. H., Thetmeyer, H., and Cromey, C. J. 2006. Settling velocity of faecal pellets of gilthead sea bream (*Sparus aurata* L.) and sea bass (*Dicentrarchus labrax* L.) and sensitivity analysis using measured data in a deposition model. *Aquaculture*, 251: 295–305.
- Marra, J. 2005. When will we tame the oceans? *Nature*, 436: 175–176.

- Mayor, D. J., Zuur, A. F., Solan, M., Paton, G. I., and Killham, K. E. N. 2010. Factors affecting benthic impacts at scottish fish farms. *Environmental Science and Technology*, 44: 2079–2084.
- McKindsey, C. W., Thetmeyer, H., Landry, T., and Silvert, W. 2006. Review of recent carrying capacity models for bivalve culture and recommendations for research and management. *Aquaculture*, 261: 451–462.
- Perez, Ó., Almansa, E., Riera, R., Rodríguez, M., Ramos, E., Costa, J., and Monterroso, O. 2014. Food and faeces settling velocities of meagre (*Argyrosomus regius*) and its application for modelling waste dispersion from sea cage aquaculture. *Aquaculture*, 420–421: 171–179.
- Plaut, I. 2001. Critical swimming speed: its ecological relevance. *Comparative Biochemistry and Physiology Part A: Molecular & Integrative Physiology*, 131: 41–50.
- R Core Team. 2018. R: A language and environment for statistical computing. R Foundation for Statistical Computing, Vienna, Austria. <http://www.r-project.org/> (last accessed 14 March 2019).
- Reid, G. K., Liutkus, M., Robinson, S. M. C., Chopin, T. R., Blair, T., Lander, T., Mullen, J., *et al.* 2009. A review of the biophysical properties of salmonid faeces: implications for aquaculture waste dispersal models and integrated multi-trophic aquaculture. *Aquaculture Research*, 40: 257–273.
- Riera, R., Pérez, Ó., Cromey, C., Rodríguez, M., Ramos, E., Álvarez, O., Domínguez, J., *et al.* 2017. MACAROMOD: a tool to model particulate waste dispersion and benthic impact from offshore sea-cage aquaculture in the Macaronesian region. *Ecological Modelling*, 361: 122–134.
- Ross, L. G., Telfer, T. C., Falconer, L., Soto, D., Aguilar-Manjarrez, J., Asmah, R., Bermúdez, J., *et al.* 2013. Carrying capacities and site selection within the ecosystem approach to aquaculture. *In Site Selection and Carrying Capacities for Inland and Coastal Aquaculture*, pp. 19–46. Ed. by L.G. Ross, T.C. Telfer, L. Falconer, D. Soto & J. Aguilar-Manjarrez. FAO/Institute of Aquaculture, University of Stirling, Expert Workshop, 6–8 December 2010. Stirl.
- SAMS. 2020. NewDEPOMOD User Guide. 132 pp. <https://depomod.sams.ac.uk/docs/UserGuide.pdf> (last accessed 30 December 2020).
- Sanchez-Jerez, P., Karakassis, I., Massa, F., Fezzardi, D., Aguilar-Manjarrez, J., Soto, D., Chapela, R., *et al.* 2016. Aquaculture's struggle for space: the need for coastal spatial planning and the potential benefits of Allocated Zones for Aquaculture (AZAs) to avoid conflict and promote sustainability. *Aquaculture Environment Interactions*, 8: 41–54.
- Sanford, L. P. 2008. Modeling a dynamically varying mixed sediment bed with erosion, deposition, bioturbation, consolidation, and armoring. *Computers and Geosciences*, 34: 1263–1283.
- SHOM. 2019. MNT, bathymétrie, Mayotte, modèle numérique de terrain. <https://diffusion.shom.fr/pro/risques/bathymetrie/mnt-fa-cade-mayotte.html> (last accessed 30 December 2020).
- Soto, D., Aguilar-Manjarrez, J., Brugère, C., Angel, D., Bailey, C., Black, K., Edwards, P., *et al.* 2008. Applying an ecosystem-based approach to aquaculture: principles, scales and some management measures. *In Building an Ecosystem Approach to Aquaculture*. FAO/Universitat de Les Illes Balears Expert Workshop. 7–11 May 2007, Palma de Mallorca, Spain, pp. 15–35. Ed. by D. Soto, J. Aguilar-Manjarrez, and N. Hishamunda. FAO Fisheries and Aquaculture Proceedings, Rome.
- Stelzenmüller, V., Gimpel, A., Gopnik, M., and Gee, K. 2017. Aquaculture site-selection and marine spatial planning: the roles of GIS-based tools and models. *In Aquaculture Perspective of Multi-Use Sites in the Open Ocean*, pp. 131–148. Springer International Publishing, Cham. http://link.springer.com/10.1007/978-3-319-51159-7_6 (last accessed 30 December 2020).
- Stigebrandt, A., Aure, J., Ervik, A., and Hansen, P. K. 2004. Regulating the local environmental impact of intensive marine fish farming. *Aquaculture*, 234: 239–261.
- Stigebrandt, A. 2011. Carrying capacity: general principles of model construction. *Aquaculture Research*, 42: 41–50.
- The Mathworks Inc. 2015. MATLAB and Statistics Toolbox Release 2015b. Natick, MA.
- Velvin, R. 1999. Environmental effects from fish farming. *In Textbook of Fish Health and Fish Diseases*, pp. 340–347. Ed. by T. Poppe. Universitetsforlaget, Oslo, Norway.
- Wang, X., Cuthbertson, A., Gualtieri, C., and Shao, D. 2020. A review on mariculture effluent: characterization and management tools. *Water*, 12: 2991.
- Weise, A. M., Cromey, C. J., Callier, M. D., Archambault, P., Chamberlain, J., and McKindsey, C. W. 2009. Shellfish-DEPOMOD: modelling the biodeposition from suspended shellfish aquaculture and assessing benthic effects. *Aquaculture*, 288: 239–253.
- Weitzman, J., and Filgueira, R. 2019. The evolution and application of carrying capacity in aquaculture: towards a research agenda. *Reviews in Aquaculture*, 12: 1–26.
- White, C. A., Nichols, P. D., Ross, D. J., and Dempster, T. 2017. Dispersal and assimilation of an aquaculture waste subsidy in a low productivity coastal environment. *Marine Pollution Bulletin*, 120: 309–321.
- White, P., and Lopez, N. A. 2017. Mariculture parks in the Philippines. *In Aquaculture Zoning, Site Selection and Area Management under the Ecosystem Approach to Aquaculture*. Full document, pp. 287–313. Ed. by J. Aguilar-Manjarrez, D. Soto & R. Brummett. Report ACS113536. Rome, FAO, and World Bank.
- Woodcock, S. H., Strohmeier, T., Strand, Ø., Olsen, S. A., and Bannister, R. J. 2018. Mobile epibenthic fauna consume organic waste from coastal fin-fish aquaculture. *Marine Environmental Research*, 137: 16–23.
- Wu, R. S. S. 1995. The environmental impact of marine fish culture: towards a sustainable future. *Marine Pollution Bulletin*, 31: 159–166.

Handling editor: Carrie Byron